Bangham CR. 2009. CTL quality and the control of human retroviral infections. Eur J Immunol 39:1700–1712.

Betts MR, Price DA, Brenchley JM, Lore K, Guenaga FJ, Smed-Sorensen A, Ambrozak DR, Migueles SA, Connors M, Roederer M, Douek DC, Koup RA. 2004. The functional profile of primary human antiviral CD8+ T cell effector activity is dictated by cognate peptide concentration. J Immunol 172:6407–6417.

Casseb J. 2009. Is human T cell lymphotropic type 1 (HTLV-1)-associated myelopathy/tropical spastic paraparesis (HAM/TSP) syndrome a neglected disease? PLoS Negl Trop Dis 3:e487.

Eiraku N, Hingorani R, Ijichi S, Machigashira K, Gregersen PK, Monteiro J, Usuku K, Yashiki S, Sonoda S, Osame M, Hall WW. 1998. Clonal expansion within CD4+ and CD8+ T cell subsets in human T lymphotropic virus type I-infected individuals. J Immunol 161:6674–6680.

Furukawa K, Mori M, Ohta N, Ikeda H, Shida H, Shiku H. 1994. Clonal expansion of CD8+ cytotoxic T lymphocytes against human T cell lymphotropic virus type I (HTLV-I) genome products in HTLV-I-associated myelopathy/tropical spastic paraparesis patients. J Clin Invest 94:1830–1839.

Gessain A, Barin F, Vernant JC, Gout O, Maurs L, Calender A, de The G. 1985. Antibodies to human T-lymphotropic virus type-I in patients with tropical spastic paraparesis. Lancet 2:407–410.

Hinuma Y, Nagata K, Hanaoka M, Nakai M, Matsumoto T, Kinoshita KI, Shirakawa S, Miyoshi I. 1981. Adult T-cell leukemia: Antigen in an ATL cell line and detection of antibodies to the antigen in human sera. Proc Natl Acad Sci USA 78:6476–6480.

Hoger TA, Jacobson S, Kawanishi T, Kato T, Nishioka K, Yamamoto K. 1997. Accumulation of human T lymphotropic virus (HTLV)-I-specific T cell clones in HTLV-I-associated myelopathy/tropical spastic paraparesis patients. J Immunol 159:2042–2048.

Ijichi S, Izumo S, Eiraku N, Machigashira K, Kubota R, Nagai M, Ikegami N, Kashio N, Umehara F, Maruyama I. 1993. An autoaggressive process against bystander tissues in HTLV-I-infected individuals: A possible pathomechanism of HAM/TSP. Med Hypotheses 41:542–547.

Itoh Y, Mizuki N, Shimada T, Azuma F, Itakura M, Kashiwase K, Kikkawa E, Kulski JK, Satake M, Inoko H. 2005. High-throughput DNA typing of HLA-A, -B, -C, and -DRB1 loci by a PCR-SSOP-Luminex method in the Japanese population. Immunogenetics 57:717–729.

Jacobson S, Shida H, McFarlin DE, Fauci AS, Koenig S. 1990. Circulating CD8+ cytotoxic T lymphocytes specific for HTLV-I pX in patients with HTLV-I associated neurological disease. Nature 348:245–248.

Jacobson S, Reuben JS, Streilein RD, Palker TJ. 1991. Induction of CD4+, human T lymphotropic virus type-1-specific cytotoxic T lymphocytes from patients with HAM/TSP. Recognition of an immunogenic region of the gp46 envelope glycoprotein of human T lymphotropic virus type-1. J Immunol 146:1155–1162.

Kannagi M, Harada S, Maruyama I, Inoko H, Igarashi H, Kuwashima G, Sato S, Morita M, Kidokoro M, Sugimoto M, Funahashi S, Osame M, Shida H. 1991. Predominant recognition of human T cell leukemia virus type I (HTLV-I) pX gene products by human CD8+ cytotoxic T cells directed against HTLV-I-infected cells. Int Immunol 3:761–767.

Kattan T, MacNamara A, Rowan AG, Nose H, Mosley AJ, Tanaka Y, Taylor GP, Asquith B, Bangham CR. 2009. The avidity and lytic efficiency of the CTL response to HTLV-1. J Immunol 182:5723–5729.

Kitze B, Usuku K, Yamano Y, Yashiki S, Nakamura M, Fujiyoshi T, Izumo S, Osame M, Sonoda S. 1998. Human CD4+ T lymphocytes recognize a highly conserved epitope of human T lymphotropic virus type 1 (HTLV-1) env gp21 restricted by HLA DRB1*0101. Clin Exp Immunol 111:278–285.

Kozako T, Arima N, Toji S, Masamoto I, Akimoto M, Hamada H, Che XF, Fujiwara H, Matsushita K, Tokunaga M, Haraguchi K, Uozumi K, Suzuki S, Takezaki T, Sonoda S. 2006. Reduced frequency, diversity, and function of human T cell leukemia virus type 1-specific CD8+ T cell in adult T cell leukemia patients. J Immunol 177:5718–5726.

Kozako T, Akimoto M, White Y, Toji S, Matsushita K, Kubota R, Izumo S, Suzuki S, Uozumi K, Shimeno H, Soeda S, Arima N. 2009a. Target epitopes of human T lymphotropic virus 1 recognized by class I MHC-restricted cytotoxic T lymphocytes in HAM/TSP patients and infected patients with autoimmune disorders. ASH Annu Meet Abstracts 114:2660.

Kozako T, Fukada K, Hirata S, White Y, Harao M, Nishimura Y, Kino Y, Soeda S, Shimeno H, Lemonnier F, Sonoda S, Arima N. 2009b. Efficient induction of human T-cell leukemia virus-1-specific CTL by chimeric particle without adjuvant as a prophylactic for adult T-cell leukemia. Mol Immunol 47:606–613.

Kozako T, Yoshimitsu M, Fujiwara H, Masamoto I, Horai S, White Y, Akimoto M, Suzuki S, Matsushita K, Uozumi K, Tei C, Arima N. 2009c. PD-1/PD-L1 expression in human T-cell leukemia virus type 1 carriers and adult T-cell leukemia/lymphoma patients. Leukemia 23:375–382.

Kubota R, Furukawa Y, Izumo S, Usuku K, Osame M. 2003. Degenerate specificity of HTLV-1-specific CD8+ T cells during viral replication in patients with HTLV-1-associated myelopathy (HAM/TSP). Blood 101:3074–3081.

Kuzushima K, Hayashi N, Kimura H, Tsurumi T. 2001. Efficient identification of HLA-A*2402-restricted cytomegalovirus-specific CD8(+) T-cell epitopes by a computer algorithm and an enzyme-linked immunospot assay. Blood 98:1872–1881.

Miyawaki S. 2000. Revised Japan criteria for Sjogren syndrome. Ryumachi 40:48–53.

Nagai M, Usuku K, Matsumoto W, Kodama D, Takenouchi N, Moritoyo T, Hashiguchi S, Ichinose M, Bangham CR, Izumo S, Osame M. 1998. Analysis of HTLV-I proviral load in 202 HAM/TSP patients and 243 asymptomatic HTLV-I carriers: High proviral load strongly predisposes to HAM/TSP. J Neurovirol 4:586–593.

Nishioka K, Maruyama I, Sato K, Kitajima I, Nakajima Y, Osame M. 1989. Chronic inflammatory arthropathy associated with HTLV-I. Lancet 1:441.

Osame M, Usuku K, Izumo S, Ijichi N, Amitani H, Igata A, Matsumoto M, Tara M. 1986. HTLV-I associated myelopathy, a new clinical entity. Lancet 1:1031–1032.

Parker CE, Daenke S, Nightingale S, Bangham CR. 1992. Activated, HTLV-1-specific cytotoxic T-lymphocytes are found in healthy seropositives as well as in patients with tropical spastic paraparesis. Virology 188:628–636.

Pique C, Saal F, Peries J, Pham D, Tursz T, Dokhelar MC. 1994. Functional comparison between HTLV-I envelopes originating from TSP/HAM or ATL cell lines. J Acquir Immune Defic Syndr 7:319–324.

Pique C, Connan F, Levilain JP, Choppin J, Dokhelar MC. 1996. Among all human T-cell leukemia virus type 1 proteins, tax, polymerase, and envelope proteins are predicted as preferential targets for the HLA-A2-restricted cytotoxic T-cell response. J Virol 70:4919–4926.

Poiesz BJ, Ruscetti FW, Gazdar AF, Bunn PA, Minna JD, Gallo RC. 1980. Detection and isolation of type C retrovirus particles from fresh and cultured lymphocytes of a patient with cutaneous T-cell lymphoma. Proc Natl Acad Sci USA 77:7415–7419.

Proietti FA, Carneiro-Proietti AB, Catalan-Soares BC, Murphy EL. 2005. Global epidemiology of HTLV-I infection and associated diseases. Oncogene 24:6058–6068.

Scherle PA, Gerhard W. 1986. Functional analysis of influenza-specific helper T cell clones in vivo. T cells specific for internal viral proteins provide cognate help for B cell responses to hemagglutinin. J Exp Med 164:1114–1128.

Silman AJ. 1988. The 1987 revised American Rheumatism Association criteria for rheumatoid arthritis. Br J Rheumatol 27:341–343.

Sonoda S, Fujiyoshi T, Yashiki S, Li HC, Lou H, Lema C. 2000. Genetic diversity of HLA in HTLV-I infection. Uirusu 50:37–45.

Sugimoto M, Nakashima H, Watanabe S, Uyama E, Tanaka F, Ando M, Araki S, Kawasaki S. 1987. T-Lymphocyte alveolitis in HTLV-I-associated myelopathy. Lancet 2:1220.

Tan EM, Cohen AS, Fries JF, Masi AT, McShane DJ, Rothfield NF, Schaller JG, Talal N, Winchester RJ. 1982. The 1982 revised criteria for the classification of systemic lupus erythematosus. Arthritis Rheum 25:1271–1277.

Terada K, Katamine S, Eguchi K, Moriuchi R, Kita M, Shimada H, Yamashita I, Iwata K, Tsuji Y, Nagataki S, Miyamoto T. 1994. Prevalence of serum and salivary antibodies to HTLV-1 in Sjogren's syndrome. Lancet 344:1116–1119.

Tsukasaki K, Hermine O, Bazarbachi A, Ratner L, Ramos JC, Harrington W, Jr., O'Mahony D, Janik JE, Bittencourt AL, Taylor GP, Yamaguchi K, Utsunomiya A, Tobinai K, Watanabe T. 2009. Definition, prognostic factors, treatment, and response criteria of adult T-cell leukemia-lymphoma: A proposal from an international consensus meeting. J Clin Oncol 27:453–459.

Ureta-Vidal A, Pique C, Garcia Z, Dehee A, Tortevoye P, Desire N, Gessain A, Chancerel B, Gout O, Lemonnier FA, Cochet M. 2001.

Human T cell leukemia virus type I (HTLV-I) infection induces greater expansions of CD8 T lymphocytes in persons with HTLV-I-associated myelopathy/tropical spastic paraparesis than in asymptomatic carriers. J Infect Dis 183:857–864.

Vernant JC, Buisson G, Magdeleine J, De Thore J, Jouannelle A, Neisson-Vernant C, Monplaisir N. 1988. T-Lymphocyte alveolitis, tropical spastic paresis, and Sjogren syndrome. Lancet 1:177.

Yamano Y, Kitze B, Yashiki S, Usuku K, Fujiyoshi T, Kaminagayoshi T, Unoki K, Izumo S, Osame M, Sonoda S. 1997. Preferential recognition of synthetic peptides from HTLV-I gp21 envelope protein by HLA-DRB1 alleles associated with HAM/TSP (HTLV-I-associated myelopathy/tropical spastic paraparesis). J Neuroimmunol 76:50–560.

Yashiki S, Fujiyoshi T, Arima N, Osame M, Yoshinaga M, Nagata Y, Tara M, Nomura K, Utsunomiya A, Hanada S, Tajima K, Sonoda S. 2001. HLA-A*26, HLA-B*4002, HLA-B*4006, and HLA-B*4801 alleles predispose to adult T cell leukemia: The limited recognition of HTLV type 1 tax peptide anchor motifs and epitopes to generate anti-HTLV type 1 tax CD8(+) cytotoxic T lymphocytes. AIDS Res Hum Retroviruses 17:1047–1061.

the FEBS Journal

Oligomannose-coated liposomes efficiently induce human T-cell leukemia virus-1-specific cytotoxic T lymphocytes without adjuvant

Tomohiro Kozako[1,2], Shinya Hirata[3], Yoshitaka Shimizu[4], Yuichiro Satoh[4], Makoto Yoshimitsu[5], Yohann White[1], François Lemonnier[6], Hiroshi Shimeno[2], Shinji Soeda[2] and Naomichi Arima[1]

1 Division of Hematology and Immunology, Center for Chronic Viral Diseases, Graduate School of Medical and Dental Sciences, Kagoshima University, Japan
2 Department of Biochemistry, Faculty of Pharmaceutical Sciences, Fukuoka University, Japan
3 Department of Immunogenetics, Graduate School of Medical Sciences, Kumamoto University, Japan
4 BioMedCore Inc., Yokohama, Kanagawa, Japan
5 Department of Hematology and Immunology, Kagoshima University Hospital, Japan
6 Unité d'Immunité Cellulaire Antivirale, Institut Pasteur, Paris, France

Keywords
adult T-cell leukemia/lymphoma; cytotoxic T lymphocytes; human T-cell leukemia virus-1; oligomannose liposome; vaccines

Correspondence
T. Kozako, Department of Biochemistry, Faculty of Pharmaceutical Sciences, Fukuoka University, 8-19-1 Nanakuma, Jonan-ku, Fukuoka 814-0180, Japan
Fax: +81 92 862 4431
Tel: +81 92 871 6631
E-mail: kozako@fukuoka-u.ac.jp
N. Arima, Division of Host Response, Center for Chronic Viral Diseases, Graduate School of Medical and Dental Sciences, Kagoshima University, 8-35-1 Sakuragaoka, Kagoshima 890-8544, Japan
Fax: +81 99 275 5947
Tel: +81 99 275 5934
E-mail: nao@m2.kufm.kagoshima-u.ac.jp

(Received 11 October 2010, revised 8 February 2011, accepted 16 February 2011)

doi:10.1111/j.1742-4658.2011.08055.x

Human T-cell leukemia virus-1 (HTLV-1) causes adult T-cell leukemia/lymphoma, which is an aggressive peripheral T-cell neoplasm. Insufficient T-cell response to HTLV-1 is a potential risk factor in adult T-cell leukemia/lymphoma. Efficient induction of antigen-specific cytotoxic T lymphocytes is important for immunological suppression of virus-infected cell proliferation and oncogenesis, but efficient induction of antigen-specific cytotoxic T lymphocytes has evaded strategies utilizing poorly immunogenic free synthetic peptides. Here, we examined the efficient induction of an HTLV-1-specific CD8+ T-cell response by oligomannose-coated liposomes (OMLs) encapsulating the human leukocyte antigen (HLA)-A*0201-restricted HTLV-1 Tax-epitope (OML/Tax). Immunization of HLA-A*0201 transgenic mice with OML/Tax induced an HTLV-1-specific gamma-interferon reaction, whereas immunization with epitope peptide alone induced no reaction. Upon exposure of dendritic cells to OML/Tax, the levels of CD86, major histocompatibility complex class I, HLA-A02 and major histocompatibility complex class II expression were increased. In addition, our results showed that HTLV-1-specific CD8+ T cells can be efficiently induced by OML/Tax from HTLV-1 carriers compared with epitope peptide alone, and these HTLV-1-specific CD8+ T cells were able to lyse cells presenting the peptide. These results suggest that OML/Tax is capable of inducing antigen-specific cellular immune responses without adjuvants and may be useful as an effective vaccine carrier for prophylaxis in tumors and infectious diseases by substituting the epitope peptide.

Abbreviations
ATL, adult T-cell leukemia/lymphoma; CFSE, 5-(and-6)-carboxy fluorescein diacetate succinimidyl ester; CTL, cytotoxic T lymphocyte; DC, dendritic cell; DPPE, dipalmitoylphosphatidylethanolamine; ELISPOT, enzyme-linked immunospot; FCM, flow cytometry; HLA, human leukocyte antigen; HTLV-1, human T-cell leukemia virus-1; iDC, immature dendritic cell; IFN-γ, interferon-gamma; IL, interleukin; Man3, mannotriose; MHC, major histocompatibility complex; MLPC, mixed lymphocyte peptide culture; OML, oligomannose-coated liposomes; PBMC, peripheral blood mononuclear cell; PBS, phosphate-buffered saline; Tgm, transgenic mice.

Introduction

Human T-cell leukemia virus-1 (HTLV-1) causes adult T-cell leukemia/lymphoma (ATL), which is an aggressive peripheral T-cell neoplasm, after a long latency period [1]. Although the process of clonal evolution of ATL cells may involve multiple steps [2], insufficient T-cell response to HTLV-1 is also a potential risk factor in ATL [3]. HTLV-1-specific cytotoxic T lymphocytes (CTLs) play a critical role in the host immune response against HTLV-1 [4,5]. We have previously reported the decreased frequency and function of HTLV-1 Tax-specific CD8+ T cells in ATL patients and have described the upregulation of the negative immunoregulatory programmed death 1 marker on HTLV-1 Tax-specific CTLs from asymptomatic HTLV-1 carriers and ATL patients [6,7]. Impaired host CTL function reduces protection against the accumulation of HTLV-1-transformed cells, and circumventing this hurdle may yield an effective immune strategy against leukemogenesis. HTLV-1 Tax-targeted vaccines in a rat model of HTLV-1-induced lymphomas showed promising antitumor effects [8]. Therefore, HTLV-1-specific CTLs are important for immunological suppression of HTLV-1-infected cell proliferation and pathogenesis of ATL. However, efficient induction of antigen-specific CTLs has evaded strategies utilizing poorly immunogenic free synthetic peptides.

Antigen-specific CTL induction is an attractive immunotherapeutic strategy against hematological malignancies, other cancers and infectious diseases [9,10]. The difficulty in inducing antigen-specific CTLs in individual patients prevents the more widespread use of adoptive T-cell therapy. Oligomannose-coated liposomes (OMLs) can be incorporated into F4/80-positive macrophages or intraperitoneal CD11b-positive dendritic cells (DCs), resulting in the induction of a protective response following injection into the peritoneal cavity [11,12]. OMLs may also activate peritoneal macrophages to upregulate the expression of costimulatory molecules and preferentially secrete interleukin-12 (IL-12), which would result in the activation of both CD4-positive and CD8-positive T cells [13]. Furthermore, OMLs employed in effective antigen delivery could induce both Th subsets and CTLs against ovalbumin antigens encapsulated in the liposomes [14]. OMLs using human monocytes/macrophages as a cellular vehicle have the potential to target peritoneal micrometastasis in the omentum of gastric cancer patients [15]. Therefore, OMLs can also be used as an effective antigen delivery system for cancer immunotherapy activating both CTLs and Th subsets [16,17].

Here we examined the efficient induction of the HTLV-1-specific CD8+ T-cell response by OMLs encapsulating the human leukocyte antigen (HLA)-A*0201-restricted HTLV-1 Tax-epitope (OML/Tax) in HLA-A*0201 transgenic mice (Tgm) and peripheral blood mononuclear cells (PBMCs) of HTLV-1 carriers. Our results indicated that HTLV-1 Tax peptide encapsulated in OMLs efficiently induced the HTLV-1-specific CD8+ T-cell response in HLA-A*0201 Tgm and HTLV-1 carriers without adjuvant, suggesting that the efficient antigen delivery system and CTL induction can be exploited to develop a prophylactic vaccine model against tumors and infectious diseases. This is the first study demonstrating the successful induction of specific CD8+ T cells against a human tumor antigen using OMLs in HLA Tgm *in vivo* and in PBMCs *ex vivo*.

Results

OML/Tax is immunogenic in the absence of adjuvant *in vivo*

To determine whether OMLs are an efficient antigen delivery system, we assessed the immune responses to OML/Tax in HLA-A*0201 Tgm following production of OMLs encapsulating the HLA-A*0201-restricted HTLV-1 Tax-epitope (Fig. 1). To determine the induction of humoral and cellular immunity for human tumor antigen, female mice were intradermally immunized twice at intervals of 14 days with OML/Tax, Tax peptide alone or phosphate-buffered saline (PBS). Seven days after the last immunization, inguinal lymph node cells from the mice immunized with these antigens were examined for their ability to induce interferon-gamma (IFN-γ)-producing cells by enzyme-linked immunospot

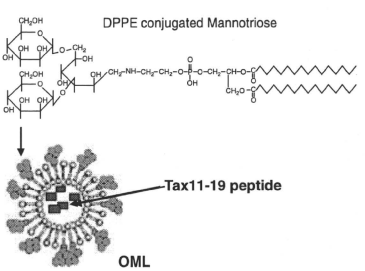

Fig. 1. Structures of synthetic neoglycolipids consisting of DPPE.

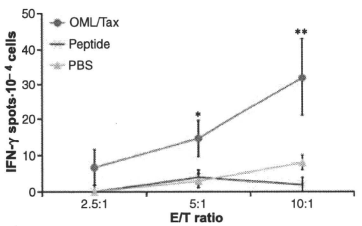

Fig. 2. Induction of cellular immunity by intradermal immunization with OML/Tax. Five HLA-A*0201 Tgm per group were intradermally immunized twice with OML/Tax, HTLV-1 peptide (LLFGYPVYV) or PBS on days 0 and 14. Seven days after the last immunization, the spleens and inguinal lymph nodes were collected. The inguinal lymph node cells (2×10^6 per well) were stimulated with HTLV-1 peptide *in vitro*. Six days later, the frequencies of cells producing IFN-γ per 2.5, 5 and 10×10^4 inguinal lymph node cells upon stimulation with syngeneic bone marrow-derived DCs (1×10^4 per well), pulsed with or without each peptide, were determined by ELISPOT assay. IFN-γ spots are expressed as the number of peptide-loaded to peptide-unloaded target cells. $^*P < 0.05$, $^{**}P < 0.01$ vs. PBS group. The experiments were carried out in triplicate. The values are the average of five mice. Results represent means ± standard deviation.

(ELISPOT) assays. Immunization of HLA-A*0201 Tgm with OML/Tax resulted in the efficient induction of IFN-γ-producing cells (Fig. 2). This induction of IFN-γ-producing cells correlated well with effector cell increases, and was significantly higher than observed for either immunization with Tax peptide alone.

To examine HTLV-1 Tax-specific CD8+ cell induction, inguinal lymph node cells from mice immunized with OML/Tax, Tax peptide alone or PBS were stimulated with Tax peptide for 32 days *in vitro*. HTLV-1 Tax-specific CD8+ cells from inguinal lymph nodes were detected using a tetramer assay. The induction of HTLV-1 Tax-specific CD8+ cells from inguinal lymph nodes was observed after immunization with OML/Tax (data not shown). The percentages of tetramer+CD8+ T cells in lymphocytes immunized with OML/Tax, Tax peptide alone or PBS were 0.12 ± 0.09, 0.06 ± 0.02 and 0.06 ± 0.05%, respectively (n = 3, mean ± standard deviations), whereas there were no significant differences between the mice immunized with OML/Tax and PBS.

Maturation of DCs through uptake of OML/Tax

DC maturation is associated with increased expression of several cell surface markers, including the costimulatory molecules CD86 and major histocompatibility complex (MHC) class II. Upon OML incorporation, IL-12 secretion and expression of costimulatory molecules, CD40, CD80, and CD86, and of MHC class II molecules were clearly enhanced on peritoneal macrophages [13]. To determine whether phenotypic maturation of DCs was mediated by OML/Tax uptake, immature DCs (iDCs) were incubated with OML/Tax for 48 h, and the expression of surface CD86, MHC class I and MHC class II was measured by flow cytometry (FCM). Upon exposure of these DCs to OML/Tax (10 $\mu g \cdot mL^{-1}$), the levels of CD86, MHC class I, HLA-A02 and MHC class II expression were increased (Table 1). As a positive control, phytohemagluttanin (PHA)-pulsed DCs also showed a marked increase, whereas HTLV-1 epitope peptide (10 $\mu g \cdot mL^{-1}$) did not upregulate these surface markers.

Table 1. Maturation of DCs through uptake of OML/Tax. Results represent means ± SD for three independent experiments. Percentage indicates mean fluorescence intensity vs. unpulsed iDC controls. $^*P < 0.05$; $^{**}P < 0.01$ vs. unpulsed iDC controls.

	OML/Tax (%)	Peptide (%)	PHA (%)
MHC Class I	208.5 ± 21.8*	129.8 ± 7.6	652.6 ± 101.4**
HLA-A02	121.0 ± 1.3*	102.7 ± 0.4	176.2 ± 3.8**
MHC Class II	115.2 ± 0.1**	103.3 ± 0.3	130.1 ± 0.4**
CD86	131.8 ± 0.4**	109.0 ± 0.1	216.9 ± 0.9**

Induction of HTLV-1 Tax-specific CD8+ T cells from HTLV-1 carriers and cytotoxic activity of induced CTLs

To examine HTLV-1 Tax-specific CD8+ cell induction in freshly isolated or cryopreserved cells from HTLV-1 carriers in mixed lymphocyte peptide culture (MLPC), PBMCs from these patients were cultured with or without 0.02 μM OML/Tax or Tax11–19 peptide followed by analysis of HTLV-1 Tax-specific CD8+ cells using the HTLV-1/HLA tetramer assay as described in the Materials and methods section. The percentage and number of tetramer+CD8+ lymphocytes were analyzed in fresh (*ex vivo*) and cultured PBMCs (Table 2). An increase in the proportion of CD8+ cells was evident for HTLV-1 carriers exposed to OML/Tax (9/10), whereas there was an increase observed in only four of 10 patients exposed to the peptide (representative data shown in Fig. 3A).

The increase in the number of tetramer+CD8+ cells was more efficient with OML/Tax (data not shown). OML/Tax increased the number of tetramer+CD8+ cells by up to 1400-fold, whereas treatment with peptide alone and with PBS alone showed increases of 95- and 35-fold, respectively. The average increase observed with

Table 2. Induction of HTLV-1 Tax-specific CD8+ T cells from HTLV-1 carriers. The tetramer assay was performed in fresh (*ex vivo*) PBMCs and on those that had been cultured for 14 days, as described in the Materials and Methods.

	Tetramer+CD8+ cells in lymphocyte (%)			
Subject No.	*ex vivo*	OML/Tax	Peptide	None
1	0.12	1.24	0.04	0.18
2	0.31	0.46	0.04	0.07
3	0.45	3.46	0.02	0.1
4	0.01	4.36	2.61	0.14
5	0	0	0.01	0
6	3.47	5.88	5.93	3.93
7	0.36	3.48	1.5	0.11
8	0.3	8.17	0.04	0.03
9	0.15	2.14	2.56	0.96
10	0.01	0.11	0.01	0.01

OML/Tax (170-fold) was significant compared with PBS alone (nine-fold). These results indicated that OML/Tax is effective for inducing tetramer + CD8 + cells in HTLV-1-infected subjects.

Furthermore, these HTLV-1-specific CD8 + cells induced apoptosis of HTLV-1 epitope peptide-pulsed T2-A2 cells (Fig. 3B). The T cells efficiently lysed Tax peptide-loaded T2-A2 cells, whereas only low-level background lysis was observed in the absence of Tax peptide, or for CMV peptide-loaded T2-A2 cells. These results indicated that the OML/Tax-induced CTL response was MHC class I restricted, specifically lysing cells presenting the appropriate peptide.

Discussion

Despite recent progress in both chemotherapy and supportive care for hematological malignancies [18–20], the prognosis of ATL is still poor; overall survival at 3 years is only 24% [21]. New strategies for the therapy and prophylaxis of ATL are still required [22]. Antigen-specific CTL induction is an attractive immunotherapeutic strategy against hematological malignancies, other cancers and infectious diseases [23,24]. Whereas free synthetic antigen peptides have proven to be relatively poor immunogens, antigen-encapsulating OMLs induce antigen-specific cell-mediated immunity that is sufficient to reject tumors or parasites [12,14,25], indicating that OMLs are useful for induction of effective cellular immunity. In this study, we demonstrated that our novel OML-based drug delivery system targeting a human tumor antigen can be used for the induction of systemic immune responses in HLA-A*0201 Tgm and HTLV-1-infected subjects.

We showed that immunization with OML/Tax induced HTLV-1-specific CD8 + cells and IFN-γ pro-

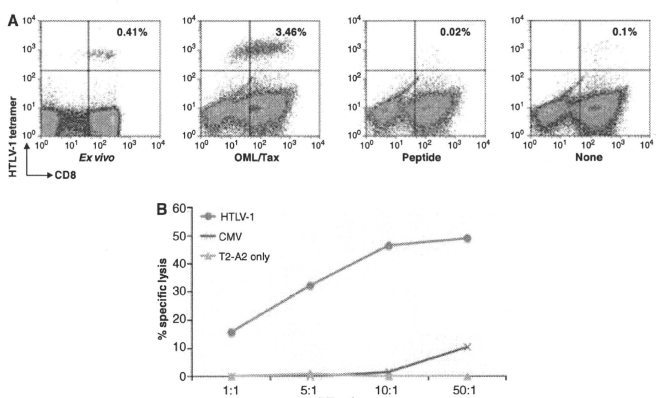

Fig. 3. Induction of HTLV-1 Tax-specific CD8+ T cells from HTLV-1 carriers. (A) Freshly isolated or cryopreserved PBMCs from HTLV-1 carriers were cultured with OML/Tax, with peptide alone or without antigen. The tetramer assay was performed in fresh (*ex vivo*) or cultured PBMCs. The numbers in the upper right quadrants represent the percentages of tetramer+CD8+ T cells in T lymphocytes. (B) Cytotoxic activity of induced HTLV-1-specific CD8+ T cells. Using HTLV-1 peptide and CMV peptide-loaded and unpulsed T2-A2 cells as target cells, specific cytotoxic activity was evaluated by FCM assay of cell-mediated cytotoxicity. All tests were carried out in triplicate at effector : target ratios of 1 : 1, 5 : 1, 10 : 1 and 50 : 1.

duction in HLA-A*0201 Tgm, whereas there was no production following immunization with epitope peptide as determined by ELISPOT. In addition, our results showed that HTLV-1-specific CD8+ cells can be efficiently induced by OML/Tax from HTLV-1 carriers compared with epitope peptide only. These results were explained by the Th1-skewing of the cytokine profiles due to the advantage of OML-mediated immunization. Mizuuchi *et al.* (H.H., Y.H., T.I., E.S., E.N., T.S. and N.S. unpublished results) have recently reported the induction of CTLs specific to the HLA-A24-restricted epitopes of Survivin2B by MLPC with OML-coated survivin2B peptide and those of human papillomavirus type16 E6 and E7 by MLPC with OML-coated papillomavirus DNA. A previous study also showed that OMLs were preferentially incorporated into macrophages [12]. As the macrophage mannose receptor (CD206) is mainly expressed on macrophages [26], the action of OMLs is thought to be caused by their facilitation of antigen delivery to macrophages as a result of interaction between CD206 and oligomannose exposed on the liposomes. In addition, a recent study showed that specific ICAM-3 grabbing nonintegrin-related 1 and complement receptor type 3 played a crucial role in the uptake of OMLs by macrophages [13]. Uptake of the HTLV-1 antigen-encapsulating OMLs by macrophages would have been an initial key event in the induction of the antigen-specific Th1 immune response. Thus, the efficient induction of HTLV-1-specific CD8+ cells by OML/Tax suggests that OMLs can be used as a novel adjuvant for efficient activation of specific cellular immunity.

Antigen-specific CTL induction is an attractive immunotherapeutic strategy against hematological malignancies, other cancers and infectious diseases [9,10]. WT1-specific tetramer+CD8+ T cells in chronic myelogenous leukemia patients inoculated with WT-1 peptide appeared in MLPC (17/20) [27]. An increase in the proportion of Tax11–19 tetramer+CD8+ cells was evident for HTLV-1 carriers exposed to OML/Tax in MLPC (9/10), compared with the increase seen for HTLV-1 carriers exposed to Tax peptide in MLPC (5/10). Half of the culture medium was changed every 2 days in MLPC. These results suggest that Tax peptides might have been taken up and presented by CD8+ T cells, which were then killed by other Tax-specific CD8+ T cells. Furthermore, not only OML/Tax but PBS alone increased the number of tetramer-plus CD8+ T cells. These results may be due to responses to the endogenous HTLV-1 Tax antigen in PBMCs.

The diversity in clinical features and prognosis of patients with this disease has led to its subclassification into the following four categories: acute, lymphoma, chronic and smoldering types. Indolent ATL (chronic and smoldering subtypes) is usually managed by careful monitoring until disease progression [18]. The median survival time of the standard treatment for aggressive ATL (acute and lymphoma types) remains inadequate. Induction of an adequate HTLV-1-specific cellular immune response may significantly reduce HTLV-1 proviral load, as reported in a squirrel monkey model of HTLV-1 infection [28]. Protection against ATL development in chronic HTLV-1 carriers may be afforded by the induction of HTLV-1-specific CTLs. Therefore, OML/Tax could be adapted as a prophylactic for acute transformation of indolent ATL. On the other hand, patients with acute- or lymphoma-type ATL are usually treated with combination chemotherapy [21]. The major obstacles in therapy are drug resistance of ATL cells to chemotherapeutic agents and the profoundly weakened and immunodeficient state of ATL patients. OML may be therapeutically useful in combination with chemotherapy.

Allogeneic stem cell transplantation has been shown to be effective in ATL patients [29], whereas patients treated with allogeneic stem cell transplantation with reduced-intensity conditioning had overall survival at 3 years of 36% [30]. Cell-mediated immunity to HTLV-1 was augmented in allogeneic stem cell transplantation patients, which might account for the efficacy of this therapy [31]. Therefore, the efficient induction of HTLV-1-specific CTL by OML/Tax could be adapted to prevent the relapse of ATL in postallogeneic stem cell transplantation patients.

The expression of Tax by the host cell targets them for attack by CTL, resulting in the elimination of the infected cell [32]. However, the expression of Tax seems to be reduced during the process of leukemogenesis [33], suggesting that Tax expression is a disadvantage for the survival of infected cells, at least in immune-competent individuals. On the other hand, ATL cells from half of the ATL cases still retain the ability to express HTLV-1 Tax, a key molecule in HTLV-1 leukemogenesis [34,35]. The CD8 cell-dependent CTLs also appear to directly target the Tax protein because when the histone deacetylase inhibitor, valproate, is used to activate tax transcription, the HTLV-1 proviral load in HAM/TSP individuals is reduced [36]. Thus, the host's CTL response could target Tax-expressing cells, thereby reducing the number of infected cells *in vivo*. In addition, the HBZ gene is expressed at a higher level [37]. The individuals with HLA class I alleles that strongly bind the HTLV-1 protein HBZ had a lower proviral load and were more likely to be asymptomatic, suggesting that HBZ plays a central role in HTLV-1 persistence. In addition, higher frequencies of both

Tax11-19- and Tax301-309-specific CTLs are related to a reduction in proviral load. Therefore, OMLs can also be used as an effective antigen delivery system for cancer immunotherapy or as a prophylactic vaccine activating both CTL and Th subsets by replacing Tax with antigens such as HBZ or tumor antigen, whereas OML/Tax could be adapted as a prophylactic for ATL and ATL patients expressing Tax.

In this study, we demonstrated that OML/Tax strongly induced the HTLV-1-specific CD8+ T-cell response without adjuvant in HLA-A*0201 Tgm and HTLV-1 carriers. These results suggest that OML/Tax is capable of inducing strong cellular immune responses, and is potentially useful as an effective prophylactic vaccine model against tumors and infectious diseases by substituting the epitope peptide.

Materials and methods

Man3–DPPE and liposome preparation

Dipalmitoylphosphatidylcholine, cholesterol and dipalmitoylphosphatidylethanolamine (DPPE) were purchased from Sigma-Aldrich (St Louis, MO, USA). Mannotriose [Man3: Mana1-6(Mana1-3)Man] was purchased from Funakoshi Co. Ltd (Tokyo, Japan). Man3–DPPE was prepared by conjugation of the Man3 with DPPE by reductive amination, as described in previous papers [38,39]. The purity of Man3–DPPE was confirmed by HPTLC (Silica gel 60 HPTLC plates; Merck, Darmstadt, Germany) and TOF MS (Auto FLEX; Bruker Daltonics, Bremen, Germany). The purified Man3–DPPE was quantified by determination of the phosphate contents. Liposomes were prepared as described previously [11,15]. Briefly, a chloroform/methanol (2 : 1, v/v) solution containing 1.5 μmol dipalmitoylphosphatidylcholine, and 1.5 μmol cholesterol was placed in a conical flask and dried by rotary evaporation. Subsequently, 2 mL ethanol containing 75 nmol Man3–DPPE and 21 μg HTLV-1 Tax11–19 peptide (LLFGYPVYV) were added to the flask and evaporated to prepare a lipid film containing Man3–DPPE and peptide. Procedures for peptide-encapsulating OMLs were as described previously [11]. The multilamellar vesicles were generated with 200 μL PBS in the dried lipid film by intense vortex dispersion. The multilamellar vesicles were extruded 10 times through polycarbonate membranes with a pore size of 1 μm (Nucleopore Track-Etched membranes; Whatman, Maidstone, Kent, UK). Liposomes entrapping peptide were separated from free untrapped peptide by four successive rounds of washing in PBS with centrifugation (20 000 ***g***, 30 min) at 4 °C. The encapsulated peptide concentration was determined by HPLC (SunFire C18 5 μm, 250 mm long × 4.6 mm ID column; Waters Corporation, Milford, MA, USA) using a gradient of 90% 1000 : 1 water/trifluoroacetic acid (solvent A)/10% 1000 : 1 acetonitrile/trifluoroacetic acid (solvent B) to 50% solvent A and 50% solvent B over 10 min, as a mobile phase.

Animals

HLA-A*0201 Tgm; H-2Db−/−β_2m−/− double knockout mice with the introduced human β_2m-HLA-A2.1 (a1 a2)-H-2Db (a3 transmembrane cytoplasmic) monochain construct gene were generated in the Department SIDA-Retrovirus, Unite d'Immunite Cellulaire Antivirale, Institut Pasteur, France [40]. Mouse experiments met with approval from the Animal Research Committee of Kumamoto University.

Induction of HTLV-1-specific CTLs in HLA-A*0201 Tgm

Five HLA-A*0201 Tgm per group were immunized intradermally via the tail on days 0 and 14 with OML/Tax (peptide content: 1 μg), Tax11-19 peptide (1 μg: LLFGYPVYV) or PBS. Cells (2×10^6 cells per well) from inguinal lymph nodes, harvested 7 days after the last immunization, were stimulated with Tax11–19 peptide *in vitro*. Six days later, the frequency of cells producing IFN-γ per 2.5, 5 and 10×10^4 inguinal lymph node cells upon stimulation with syngeneic bone marrow-derived DCs (1×10^4 cells per well) [41] (pulsed with or without HTLV-1 Tax peptide) was assayed by ELISPOT using the ELISPOT Set (BD Biosciences, San Jose, CA, USA) as described previously [42].

Maturation of DCs

Murine iDCs were obtained from bone marrow precursors using the method described previously [41].

FCM

Phenotypic analysis using HTLV-1 Tax11-19 (LLFGYPVYV)/HLA-A*0201 tetramers (Medical and Biological Laboratories, Nagoya, Japan) was performed by FCM as described previously [6,43,44]. Briefly, aliquots of 1×10^6 freshly isolated, cryopreserved or cultured cells were incubated with the HLA tetramers, fluorescein isothiocyanate-conjugated anti-human CD8 IgG (clone: T8; Beckman Coulter Co., Fullerton, CA, USA), fluorescein isothiocyanate-conjugated anti-mouse CD8 IgG_{2A} (clone: Ly-2; BD Biosciences) or 7-amino-actinomycin D (Beckman Coulter Co.). Tetramer-positive CD8+ lymphocytes and 7-amino-actinomycin D-negative viable cells were analyzed using a FACScan instrument (BD Biosciences) and FLOWJO software (Tree Star, San Carlos, CA, USA). Mature DCs were immunostained with anti-mouse CD86 (clone: GL1; BD PharMingen, San Diego, CA, USA), anti-mouse MHC class II (clone: NIMR-4; eBioscience, San Diego, CA, USA), anti-mouse MHC class I (clone: 34-1-2S; eBioscience) and

anti-HLA-A02 (clone: BB7.2; Santa Cruz Biotechnology, Santa Cruz, CA, USA) IgG_{2A} as maturation markers by FCM on a FACScan (BD Biosciences). The data are expressed as mean fluorescence intensity compared with unpulsed iDC controls.

Clinical samples

The subjects in this study included 10 HTLV-1 carriers, all of whom were recruited from patients at Kagoshima University Hospital. The subjects were examined by standard serological testing for the presence of HTLV-1 and by hematological/southern blot analysis for the diagnosis of ATL. All subjects gave their written informed consent for participation in this study and to allow review of their medical records, and provided a sample of PBMCs for HLA typing and for the HLA tetramer assay [6]. The study protocol was reviewed and approved by the Medical Ethics Committee of Kagoshima University.

Preparation of PBMCs

PBMCs were obtained from peripheral blood by separation on Ficoll/Hypaque (Pharmacia, Uppsala, Sweden) density gradient centrifugation at 400 *g* for 30 min, followed by washing three times by centrifugation with 1% fetal bovine serum RPMI-1640 at 200 *g* for 10 min to remove residual platelets. The fresh PBMCs were used for the tetramer assay and *ex vivo* expansion of anti-HTLV-1 CD8+ CTL. The remaining PBMCs were cryopreserved in liquid nitrogen until examination, as described previously [6].

Induction of HTLV-1 Tax-specific CD8+ T cells from HTLV-1 carriers

Aliquots of PBMCs (1×10^6 cells) were used for *in vitro* expansion of HTLV-1-specific CD8+ T cell clones in culture with each antigen in RPMI-1640 medium supplemented with the following reagents: 100 $U \cdot mL^{-1}$ penicillin, 0.1 $mg \cdot mL^{-1}$ streptomycin, 0.1 mM nonessential amino acids, 2 mM L-glutamine, 1 mM sodium pyruvate, 0.05 mM 2-mercaptoethanol, 50 $U \cdot mL^{-1}$ recombinant human IL-2 and 10% heat-inactivated fetal bovine serum (RPMI-1640-CM). Half of the culture medium was removed every 2 days and replaced with RPMI-1640-CM. All culture conditions were as described elsewhere [6] in a modification of the method described by Karanikas *et al.* [45]. The PBMCs cultured for 14 days were examined using the HTLV-1/HLA tetramer assay described above [6].

FCM assay of cell-mediated cytotoxicity

Cytotoxic activity of peptide-specific CTLs was evaluated as described previously [43,46]. Briefly, T2-A2 cells, *HLA-A*0201*-transfected, transporter associated with antigen processing-deficient (T × B) cell hybrid T2 cell line, were incubated at 26 °C for 16 h, then incubated with/without HLA-A*0201-restricted HTLV-1 Tax peptide (LLFGYPVYV: 10 μM) or HLA-A*0201-restricted CMV pp65 peptide (NLVPMVATV: 10 μM) for 2 h at 26 °C followed by labeling with 5-(and-6)-carboxy fluorescein diacetate succinimidyl ester (CFSE; Wako, Osaka, Japan). CFSE-labeled target cells were washed three times and seeded in 96-well plates at a concentration of 1×10^4 cells per well. CTLs were added at effector : target cell ratios of 1 : 1, 5 : 1, 10 : 1 and 50 : 1 and incubated at 37 °C for 4 h. All tests were performed in triplicate. Cytotoxicity (%) = $[(ET - T0)/(100 - T0)] \times 100$; ET = Annexin V-PE-Cy5 (Medical and Biological Laboratories) positive rate in the CFSE-positive cells when target cells were cocultured with effector cells. T0 = Annexin V positive rate in the CFSE-positive cells when target cells were not cocultured with effector cells.

Statistical analysis

Data obtained by FCM and ELISPOT assay were analyzed using a two-tailed Student's *t* test. In all analyses, $P < 0.05$ was taken to indicate statistical significance. Statistical analyses were performed using the STATVIEW 5.0 software package (Abacus Concepts, Calabasas, CA, USA).

Acknowledgements

This work was supported in part by a Grant-in-Aid for Scientific Research (to NA and TK) from the Japanese Ministry of Health, Labour, and Welfare, by the Kagoshima University for Frontier Science Research Center Program (to NA) and by Japan Leukemia Research Fund (to TK).

References

1 Uchiyama T (1997) Human T cell leukemia virus type I (HTLV-I) and human diseases. *Annu Rev Immunol* **15**, 15–37.
2 Yoshida M (2010) Molecular approach to human leukemia: isolation and characterization of the first human retrovirus HTLV-1 and its impact on tumorigenesis in adult T-cell leukemia. *Proc Jpn Acad Ser B Phys Biol Sci* **86**, 117–130.
3 Yasunaga J & Matsuoka M (2007) Leukaemogenic mechanism of human T-cell leukaemia virus type I. *Rev Med Virol* **17**, 301–311.
4 Jacobson S, Shida H, McFarlin DE, Fauci AS & Koenig S (1990) Circulating CD8+ cytotoxic T lymphocytes specific for HTLV-I pX in patients with HTLV-I associated neurological disease. *Nature* **348**, 245–248.

5 Bangham CR (2008) HTLV-1 infection: role of CTL efficiency. *Blood* **112**, 2176–2177.
6 Kozako T, Arima N, Toji S, Masamoto I, Akimoto M, Hamada H, Che XF, Fujiwara H, Matsushita K, Tokunaga M *et al.* (2006) Reduced frequency, diversity, and function of human T cell leukemia virus type 1-specific CD8+ T cell in adult T cell leukemia patients. *J Immunol* **177**, 5718–5726.
7 Kozako T, Yoshimitsu M, Fujiwara H, Masamoto I, Horai S, White Y, Akimoto M, Suzuki S, Matsushita K, Uozumi K *et al.* (2009) PD-1/PD-L1 expression in human T-cell leukemia virus type 1 carriers and adult T-cell leukemia/lymphoma patients. *Leukemia* **23**, 375–382.
8 Ohashi T, Hanabuchi S, Kato H, Tateno H, Takemura F, Tsukahara T, Koya Y, Hasegawa A, Masuda T & Kannagi M (2000) Prevention of adult T-cell leukemia-like lymphoproliferative disease in rats by adoptively transferred T cells from a donor immunized with human T-cell leukemia virus type 1 Tax-coding DNA vaccine. *J Virol* **74**, 9610–9616.
9 Albert ML, Sauter B & Bhardwaj N (1998) Dendritic cells acquire antigen from apoptotic cells and induce class I-restricted CTLs. *Nature* **392**, 86–89.
10 Kawakami Y, Fujita T, Kudo C, Sakurai T, Udagawa M, Yaguchi T, Hasegawa G, Hayashi E, Ueda Y, Iwata T *et al.* (2008) Dendritic cell based personalized immunotherapy based on cancer antigen research. *Front Biosci* **13**, 1952–1958.
11 Ikehara Y, Niwa T, Biao L, Ikehara SK, Ohashi N, Kobayashi T, Shimizu Y, Kojima N & Nakanishi H (2006) A carbohydrate recognition-based drug delivery and controlled release system using intraperitoneal macrophages as a cellular vehicle. *Cancer Res* **66**, 8740–8748.
12 Shimizu Y, Takagi H, Nakayama T, Yamakami K, Tadakuma T, Yokoyama N & Kojima N (2007) Intraperitoneal immunization with oligomannose-coated liposome-entrapped soluble leishmanial antigen induces antigen-specific T-helper type immune response in BALB/c mice through uptake by peritoneal macrophages. *Parasite Immunol* **29**, 229–239.
13 Takagi H, Furuya N & Kojima N (2007) Preferential production of IL-12 by peritoneal macrophages activated by liposomes prepared from neoglycolipids containing oligomannose residues. *Cytokine* **40**, 241–250.
14 Ikehara Y, Shiuchi N, Kabata-Ikehara S, Nakanishi H, Yokoyama N, Takagi H, Nagata T, Koide Y, Kuzushima K, Takahashi T *et al.* (2008) Effective induction of anti-tumor immune responses with oligomannose-coated liposome targeting to intraperitoneal phagocytic cells. *Cancer Lett* **260**, 137–145.
15 Matsui M, Shimizu Y, Kodera Y, Kondo E, Ikehara Y & Nakanishi H (2010) Targeted delivery of oligomannose-coated liposome to the omental micrometastasis by peritoneal macrophages from patients with gastric cancer. *Cancer Sci* **101**, 1670–1677.
16 Fukasawa M, Shimizu Y, Shikata K, Nakata M, Sakakibara R, Yamamoto N, Hatanaka M & Mizuochi T (1998) Liposome oligomannose-coated with neoglycolipid, a new candidate for a safe adjuvant for induction of CD8+ cytotoxic T lymphocytes. *FEBS Lett* **441**, 353–356.
17 Sugimoto M, Ohishi K, Fukasawa M, Shikata K, Kawai H, Itakura H, Hatanaka M, Sakakibara R, Ishiguro M, Nakata M *et al.* (1995) Oligomannose-coated liposomes as an adjuvant for the induction of cell-mediated immunity. *FEBS Lett* **363**, 53–56.
18 Tsukasaki K, Hermine O, Bazarbachi A, Ratner L, Ramos JC, Harrington W Jr, O'Mahony D, Janik JE, Bittencourt AL, Taylor GP *et al.* (2009) Definition, prognostic factors, treatment, and response criteria of adult T-cell leukemia-lymphoma: a proposal from an international consensus meeting. *J Clin Oncol* **27**, 453–459.
19 Uozumi K (2010) Treatment of adult T-cell leukemia. *J Clin Exp Hematop* **50**, 9–25.
20 Bazarbachi A, Plumelle Y, Carlos Ramos J, Tortevoye P, Otrock Z, Taylor G, Gessain A, Harrington W, Panelatti G & Hermine O (2010) Meta-analysis on the use of zidovudine and interferon-alfa in adult T-cell leukemia/lymphoma showing improved survival in the leukemic subtypes. *J Clin Oncol* **28**, 4177–4183.
21 Tsukasaki K, Utsunomiya A, Fukuda H, Shibata T, Fukushima T, Takatsuka Y, Ikeda S, Masuda M, Nagoshi H, Ueda R *et al.* (2007) VCAP-AMP-VECP compared with biweekly CHOP for adult T-cell leukemia-lymphoma: Japan Clinical Oncology Group Study JCOG9801. *J Clin Oncol* **25**, 5458–5464.
22 Matsuoka M & Jeang KT (2007) Human T-cell leukaemia virus type 1 (HTLV-1) infectivity and cellular transformation. *Nat Rev Cancer* **7**, 270–280.
23 Brown PH, Viner JL, Brewster A, Heckman CJ, Hursting S, Johnson K & Mao JT (2009) Conference report: Seventh Annual AACR International Conference on Frontiers in Cancer Prevention Research. *Cancer Prev Res (Phila Pa)* **2**, 995–998.
24 Beatty PL, Narayanan S, Gariepy J, Ranganathan S & Finn OJ (2010) Vaccine against MUC1 antigen expressed in inflammatory bowel disease and cancer lessens colonic inflammation and prevents progression to colitis-associated colon cancer. *Cancer Prev Res (Phila Pa)* **3**, 438–446.
25 Kojima N, Biao L, Nakayama T, Ishii M, Ikehara Y & Tsujimura K (2008) Oligomannose-coated liposomes as a therapeutic antigen-delivery and an adjuvant vehicle for induction of *in vivo* tumor immunity. *J Control Release* **129**, 26–32.
26 East L & Isacke CM (2002) The mannose receptor family. *Biochim Biophys Acta* **1572**, 364–386.

27 Narita M, Masuko M, Kurasaki T, Kitajima T, Takenouchi S, Saitoh A, Watanabe N, Furukawa T, Toba K, Fuse I *et al.* (2010) WT1 peptide vaccination in combination with imatinib therapy for a patient with CML in the chronic phase. *Int J Med Sci* **7**, 72–81.

28 Kazanji M, Heraud JM, Merien F, Pique C, de The G, Gessain A & Jacobson S (2006) Chimeric peptide vaccine composed of B- and T-cell epitopes of human T-cell leukemia virus type 1 induces humoral and cellular immune responses and reduces the proviral load in immunized squirrel monkeys (*Saimiri sciureus*). *J Gen Virol* **87**, 1331–1337.

29 Utsunomiya A, Miyazaki Y, Takatsuka Y, Hanada S, Uozumi K, Yashiki S, Tara M, Kawano F, Saburi Y, Kikuchi H *et al.* (2001) Improved outcome of adult T cell leukemia/lymphoma with allogeneic hematopoietic stem cell transplantation. *Bone Marrow Transplant* **27**, 15–20.

30 Tanosaki R, Uike N, Utsunomiya A, Saburi Y, Masuda M, Tomonaga M, Eto T, Hidaka M, Harada M, Choi I *et al.* (2008) Allogeneic hematopoietic stem cell transplantation using reduced-intensity conditioning for adult T cell leukemia/lymphoma: impact of antithymocyte globulin on clinical outcome. *Biol Blood Marrow Transplant* **14**, 702–708.

31 Okamura J, Uike N, Utsunomiya A & Tanosaki R (2007) Allogeneic stem cell transplantation for adult T-cell leukemia/lymphoma. *Int J Hematol* **86**, 118–125.

32 Satou Y & Matsuoka M (2010) HTLV-1 and the host immune system: how the virus disrupts immune regulation, leading to HTLV-1 associated diseases. *J Clin Exp Hematop* **50**, 1–8.

33 Furukawa Y, Osame M, Kubota R, Tara M & Yoshida M (1995) Human T-cell leukemia virus type-1 (HTLV-1) Tax is expressed at the same level in infected cells of HTLV-1-associated myelopathy or tropical spastic paraparesis patients as in asymptomatic carriers but at a lower level in adult T-cell leukemia cells. *Blood* **85**, 1865–1870.

34 Harashima N, Kurihara K, Utsunomiya A, Tanosaki R, Hanabuchi S, Masuda M, Ohashi T, Fukui F, Hasegawa A, Masuda T *et al.* (2004) Graft-versus-Tax response in adult T-cell leukemia patients after hematopoietic stem cell transplantation. *Cancer Res* **64**, 391–399.

35 Kannagi M, Harashima N, Kurihara K, Ohashi T, Utsunomiya A, Tanosaki R, Masuda M, Tomonaga M & Okamura J (2005) Tumor immunity against adult T-cell leukemia. *Cancer Sci* **96**, 249–255.

36 Lezin A, Gillet N, Olindo S, Signate A, Grandvaux N, Verlaeten O, Belrose G, de Carvalho Bittencourt M, Hiscott J, Asquith B *et al.* (2007) Histone deacetylase mediated transcriptional activation reduces proviral loads in HTLV-1 associated myelopathy/tropical spastic paraparesis patients. *Blood* **110**, 3722–3728.

37 Macnamara A, Rowan A, Hilburn S, Kadolsky U, Fujiwara H, Suemori K, Yasukawa M, Taylor G, Bangham CR & Asquith B (2010) HLA class I binding of HBZ determines outcome in HTLV-1 infection. *PLoS Pathog* **6**, el001117.

38 Shimizu Y, Yamakami K, Gomi T, Nakata M, Asanuma H, Tadakuma T & Kojima N (2003) Protection against Leishmania major infection by oligomannose-coated liposomes. *Bioorg Med Chem* **11**, 1191–1195.

39 Kato C, Kajiwara T, Numazaki M, Takagi H & Kojima N (2008) Oligomannose-coated liposomes activate ERK via Src kinases and PI3K/Akt in J774A.1 cells. *Biochem Biophys Res Commun* **372**, 898–901.

40 Pascolo S, Bervas N, Ure JM, Smith AG, Lemonnier FA & Perarnau B (1997) HLA-A2.1-restricted education and cytolytic activity of CD8(+) T lymphocytes from beta2 microglobulin (beta2m) HLA-A2.1 monochain transgenic H-2Db beta2m double knockout mice. *J Exp Med* **185**, 2043–2051.

41 Senju S, Hirata S, Matsuyoshi H, Masuda M, Uemura Y, Araki K, Yamamura K & Nishimura Y (2003) Generation and genetic modification of dendritic cells derived from mouse embryonic stem cells. *Blood* **101**, 3501–3508.

42 Komori H, Nakatsura T, Senju S, Yoshitake Y, Motomura Y, Ikuta Y, Fukuma D, Yokomine K, Harao M, Beppu T *et al.* (2006) Identification of HLA-A2- or HLA-A24-restricted CTL epitopes possibly useful for glypican-3-specific immunotherapy of hepatocellular carcinoma. *Clin Cancer Res* **12**, 2689–2697.

43 Kozako T, Fukada K, Hirata S, White Y, Harao M, Nishimura Y, Kino Y, Soeda S, Shimeno H, Lemonnier F *et al.* (2009) Efficient induction of human T-cell leukemia virus-1-specific CTL by chimeric particle without adjuvant as a prophylactic for adult T-cell leukemia. *Mol Immunol* **47**, 606–613.

44 Kozako T, Akimoto M, Toji S, White Y, Suzuki S, Arima T, Suruga Y, Matsushita K, Shimeno H, Soeda S *et al.* (2011) Target epitopes of HTLV-1 recognized by class I MHC-restricted cytotoxic T lymphocytes in patients with myelopathy and spastic paraparesis and infected patients with autoimmune disorders. *J Med Virol* **83**, 501–509.

45 Karanikas V, Lurquin C, Colau D, van Baren N, De Smet C, Lethe B, Connerotte T, Corbiere V, Demoitie MA, Lienard D *et al.* (2003) Monoclonal anti-MAGE-3 CTL responses in melanoma patients displaying tumor regression after vaccination with a recombinant canarypox virus. *J Immunol* **171**, 4898–4904.

46 Aubry JP, Blaecke A, Lecoanet-Henchoz S, Jeannin P, Herbault N, Caron G, Moine V & Bonnefoy JY (1999) Annexin V used for measuring apoptosis in the early events of cellular cytotoxicity. *Cytometry* **37**, 197–204.

Bioorganic & Medicinal Chemistry 18 (2010) 2402–2411

Contents lists available at ScienceDirect

Bioorganic & Medicinal Chemistry

journal homepage: www.elsevier.com/locate/bmc

Structural development studies of anti-hepatitis C virus agents with a phenanthridinone skeleton

Masahiko Nakamura [a], Atsushi Aoyama [a], Mohammed T. A. Salim [b], Mika Okamoto [b], Masanori Baba [b,*], Hiroyuki Miyachi [c], Yuichi Hashimoto [a], Hiroshi Aoyama [a,*]

[a] Institute of Molecular & Cellular Biosciences, The University of Tokyo, 1-1-1 Yayoi, Bunkyo-ku, Tokyo 113-0032, Japan
[b] Division of Antiviral Chemotherapy, Center for Chronic Viral Diseases, Graduate School of Medical and Dental Sciences, Kagoshima University, 8-35-1 Sakuragaoka, Kagoshima 890-8544, Japan
[c] Division of Pharmaceutical Sciences, Okayama University Graduate School of Medicine, Dentistry and Pharmaceutical Sciences, 1-1-1 Tsushima-Naka, Kita-ku, Okayama 700-8530, Japan

ARTICLE INFO

Article history:
Received 10 February 2010
Revised 24 February 2010
Accepted 25 February 2010
Available online 2 March 2010

Keywords:
Anti-HCV agents
Phenanthridinone
Thalidomide
Am80
Am580

ABSTRACT

A phenanthridinone skeleton was derived from our previous researches on thalidomide and retinoids as a multi-template for generation of anti-viral lead compounds. Structural development studies focusing on anti-hepatitis C virus activity afforded 5-butyl-2-(1,1,1,3,3,3-hexafluoro-2-hydroxypropan-2-yl)phenanthridin-6(5*H*)-one (**10**) and 5-butylbenzo[*b*]phenanthridin-6(5*H*)-one (**39**), which showed EC_{50} values of approximately 3.7 and 3.2 μM, respectively.

1. Introduction

The efficient identification of small-molecular scaffolds for the development of biologically active compounds is very important in chemical genetics and medicinal chemistry. As one approach, we have been utilizing the multi-template hypothesis,[1–5] based on the idea that the number of protein fold structure types that comprise all the domains occurring in natural proteins is quite limited, in spite of the huge number of natural proteins.[6–8] A given fold structure might be characteristic of many natural proteins, and therefore, ignoring physical/chemical interactions, one might expect that a template/scaffold structure which is spatially complementary to one fold structure might serve as a multi-template for structural development of ligands that would interact specifically with many different natural proteins. As candidate multi-template structures, we have focused particularly on thalidomide (**1**) and retinoids, including synthetic retinoids Am80 (**2**) and Am580 (**3**) (Fig. 1).[1,9–13] All of these compounds **1**–**3** elicit a wide range of biological activities, and thalidomide (**1**) is well-established to be multi-target drug.[1,9–13] In fact, we recently applied thalidomide (**1**) and/or Am80 (**2**)/Am580 (**3**) as multi-templates to develop anti-viral agents and/or anti-proliferative agents for virus-infected cells, that is, anti-bovine viral diarrhea virus (anti-BVDV) agents, including SK3M4M5M (**4**) derived from thalidomide (**1**)[14,15] and adult T-cell leukemia (ATL) cell-selective proliferation inhibitors, including TMN($COCH_3$) (**5**) and TMN(OH)($COCH_3$) (**6**) derived from Am80 (**2**)/Am580 (**3**) (Fig. 1).[4] We next aimed to develop anti-hepatitis C virus (HCV) agents.

HCV infection is thought to be a major cause of human hepatitis,[16,17] and it is estimated that at least 170 million people worldwide are chronically infected with this virus.[18] Most infections become persistent and about 60% of cases progress to chronic liver disease, which in turn can lead to development of cirrhosis, hepatocellular carcinoma, and liver failure.[19,20] Currently, no vaccine is available against HCV infection, and the standard treatment for chronic hepatitis C consists of pegylated interferon (IFN)-α in combination with the nucleoside analog ribavirin (1-β-D-ribofuranosyl-1,2,4-triaxole-3-carboxamide). However, the virus cannot be eliminated from approximately half of infected patients treated with these agents.[21] In addition, the side effects of these agents are sometimes serious and unacceptable to patients. Therefore, alternative agents for the treatment and prevention of HCV infection are urgently needed.

As mentioned above, we have been succeeded in the development of potent anti-BVDV agents, including SK3M4M5M (**4**), which

* Corresponding authors. Tel.: +81 3 5841 7848; fax: +81 5841 8495 (H.A.); tel.: +81 99 275 5930; fax: +81 99 275 5932 (M.B.).
E-mail addresses: m-baba@vanilla.ocn.ne.jp (M. Baba), aoyama@iam.u-tokyo.ac.jp (H. Aoyama).

0968-0896/$ - see front matter © 2010 Elsevier Ltd. All rights reserved.
doi:10.1016/j.bmc.2010.02.057

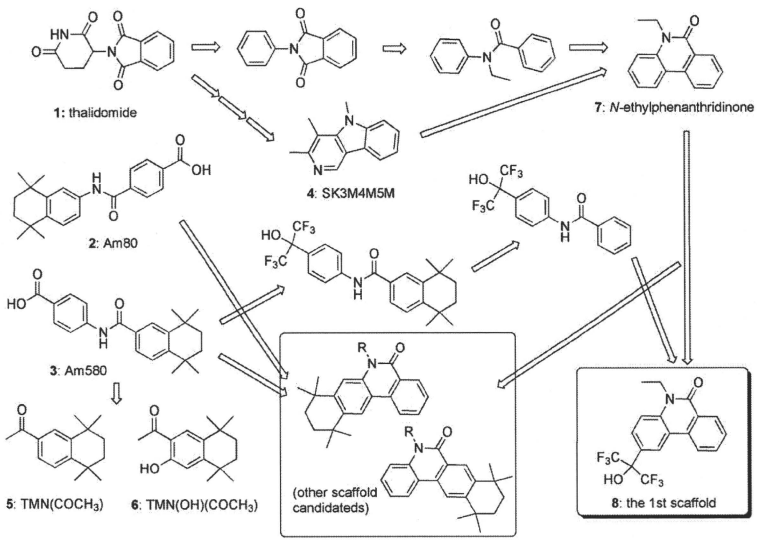

Figure 1. Armchair structural development of thalidomide (**1**) and retinoids (**2**, **3**) to the first scaffold **8**.

have an EC_{50} value of 3.5 nM.[15] Although BVDV belongs to the *Flaviviridae* family, as HCV does,[22] and is thought to be a surrogate model for HCV,[23–25] SK3M4M5M (**4**) showed only a very weak activity against HCV. Therefore, we tried to develop another scaffold for the development of anti-HCV agents, as shown in Figure 1.

2. Results and discussion

2.1. Armchair structural development leading to phenanthridinone derivatives

First, we applied armchair structural development to phenylphthalimide, which was itself developed from thalidomide (**1**). The phenylphthalimide skeleton is a superior multi-template, and we have developed various biologically active phenylphthalimide derivatives, including tumor necrosis factor-α production regulators, tubulin polymerization inhibitors, dipeptidylpeptidase type IV inhibitors, liver X receptor antagonists, α-glucosidase inhibitors, and so on.[1,9–12] The armchair ring opening of phenylphthalimide gave *N*-ethylbenzanilide, whose recyclization should afford *N*-ethylphenanthridinone (**7**) (Fig. 1). On the other hand, synthetic retinoids Am80 (**2**) and Am580 (**3**) both possess a benzoic acid moiety. Because our previous studies on anti-BVDV agents suggested that carboxyl acid derivatives are not suitable as lead structures, we considered that a bioisosteric functional group, the 1,1,1,3,3,3-hexafluoropropan-2-ol-substituted phenyl moiety, might be introduced into *N*-ethylphenanthridinone (**7**) to give the first scaffold structure, 5-ethyl-2-(1,1,1,3,3,3-hexafluoro-2-hydroxypropan-2-yl) phenanthridin-6(5*H*)-one (**8**) (Fig. 1). In addition, both Am80 (**2**) and Am580 (**3**) possess a teterahydrotetramethylnaphthalene moiety, which has been established to be a useful core structure to develop ATL cell-selective proliferation inhibitors, including $TMN(COCH_3)$ (**5**) and $TMN(OH)(COCH_3)$ (**6**).[4] We therefore considered that docking of teterahydrotetramethylnaphthalene moiety and *N*-ethylphenanthridinone (**7**) would afford other scaffold candidate structures, as shown in Figure 1.

Compound **8** was prepared as shown in Scheme 1.[26,27] Briefly, *N*-ethylaniline was treated with hexafluoroacetone to give the 1,1,1,3,3,3-hexafluoro-2-hydroxypropyl derivative, which was coupled with 2-iodobenzoyl chloride. The resulting anilide was cyclized to give compound **8**. The anti-HCV activity of compound **8** was determined in the established HCV RNA replicon cells.[28] Briefly, NNC #2 cells carrying full-genomic HCV RNA replicons were cultured in the presence of various concentrations of the test compounds for 3 days. The cells were examined for HCV RNA and glyceraldehyde-3-phosphate dehydrogenase (GAPDH) RNA levels by real-time reverse transcription (RT)-PCR. The anti-HCV activity and cytotoxicity of test compounds were expressed as 50% effective concentration (EC_{50}) and 50% cytotoxic concentration (CC_{50}), defined in terms of decrease of HCV RNA and GAPDH RNA levels to 50% of the respective control levels. As shown in Figure 2, compound **8** showed apparent anti-HCV activity (EC_{50} and CC_{50}: 14.1 and >40 μM, respectively), suggesting that compound **8** could be a lead compound for structural development of anti-HCV agents.

2.2. Effects of N-substituents

Since compound **8** showed anti-HCV activity, we examined the effects of *N*-substituents. Several N-alkylated derivatives of **8** (**9**–**14**) were prepared as shown in Scheme 2, and their anti-HCV activity was measured as described above (Figs. 2 and 3).

As shown in Figures 2 and 3, introduction of three fluorine atoms at the terminal methyl group (**9**) did not improve the activity. However, introduction of a longer-chain alkyl group, *n*-butyl (**10**), *n*-hexyl (**11**), or *n*-nonyl (**12**), resulted in enhancement of anti-HCV activity, though at the same time, the cytotoxicity was increased. The anti-HCV activity of these compounds decreased

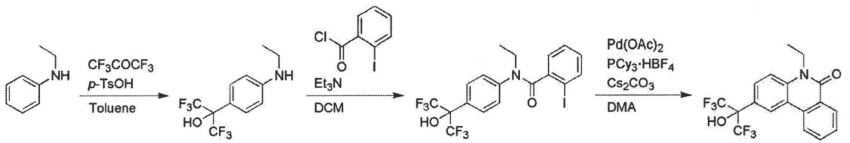

Scheme 1.

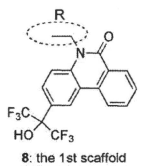

R	EC_{50} (μM)	CC_{50} (μM)
8: CH_3CH_2-	14.1	>40
9: CF_3CH_2-	24.8	30.3
10: $CH_3(CH_2)_3$-	3.7	12.5
11: $CH_3(CH_2)_5$-	4.8	12.2
12: $CH_3(CH_2)_8$-	8.3	10.2
13: $PhCH_2$-	7.7	18.2
14: c-$C_6H_{11}CH_2$-	6.7	14.4

Figure 2. Effects of N-substituents on anti-HCV activity. EC_{50}: 50% effective concentration, based on the decrease of the amount of HCV RNA. CC_{50}: 50% cytotoxic concentration, based on the decrease of the amount of GAPDH RNA.

in the order of: **10** > **11** > **12**. On the other hand, their cytotoxicity tended to decrease in the reverse order, though the differences were small. The benzyl analog (**13**) and the cyclohexylmethyl analog (**14**) showed moderate anti-HCV activity (EC_{50}: 7.7 and 6.7 μM, respectively) with weaker cytotoxicity (CC_{50}: 18.2 and 14.4 μM, respectively). Cytotoxicity was not affected by the length of the introduced alkyl group (CC_{50}: 10.2–12.5 μM). Among this series, compound **10** showed the most potent anti-HCV activity (EC_{50}: 3.7 μM). Therefore, we selected the *N*-butylphenanthridinone skeleton (corresponding to compound **10**) as a scaffold structure for further structural development studies.

2.3. Regioisomers of methyl-substituted *N*-butylphenanthridinone

Based on our previous structure–activity relationship studies of anti-BVDV γ-carboline analogs, which indicated that regio-selective methyl-substitution dramatically influenced the anti-viral activity,[14,15] the effect of methyl-substitution was investigated. For this purpose, we synthesized all the regioisomers of methyl-

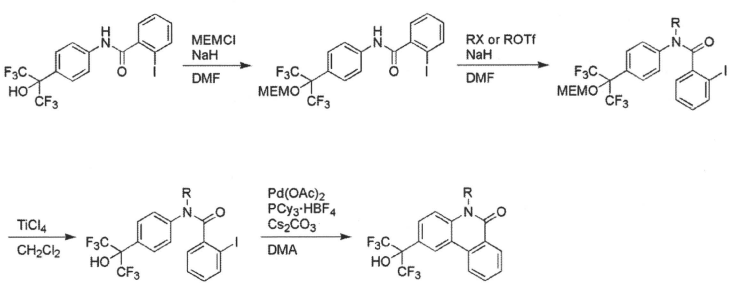

Scheme 2.

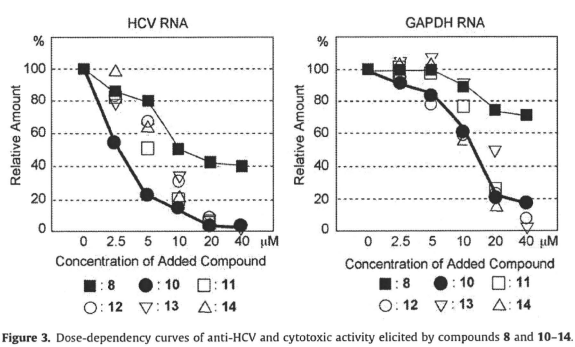

Figure 3. Dose-dependency curves of anti-HCV and cytotoxic activity elicited by compounds **8** and **10–14**.

substituted *N*-butylphenanthridinone (Fig. 4) by the method shown in Scheme 3.

As shown in Figure 4, *N*-butylphenanthridinone itself (an extracted structure from compound **10**) was completely inactive. However, methyl-substitution at position 2, that is, the position at which the 1,1,1,3,3,3-hexafluoropropan-2-ol group was attached in compound **10**, resulted in the appearance of anti-HCV activity (EC_{50}: 42.0 μM). All the other regioisomers, except the 8-methyl analog (**21**), that is, compounds **16**, **18–20**, **22**, and **23**, were inactive, and the anti-HCV activity elicited by **21** was very weak. Therefore, position 2 seems to be the best position at which to introduce a substituent.

2.4. Effect of 2-subsituents on anti-HCV activity

The results described above prompted us to examine the effect of 2-substitutents, and we prepared various derivatives (**24–33**) as shown in Figure 5. Although some derivatives, including compounds **28–33**, showed improved anti-HCV activity compared to the 2-methyl analog **17**, their activity was weaker than that of **10**. As already mentioned, the unsubstituted analog **15** was inactive. Its fluoro analog **24** was also inactive, suggesting that a mono-atomic substituent is inappropriate to improve the activity. Though the 2-methyl analog **17** showed some activity (EC_{50}: 35.8 μM), its trifluoromethyl analog **26** was inactive. On the contrary, its hydroxyl analog **25** showed activity comparable to that of the 2-methyl analog **17**. The 2-ethyl analog **27** also showed activity comparable to that of **17**/**25**.

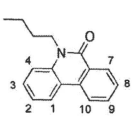

%-Inhibition of HCV gene and host cell gene (GAPDH) expression at 10 μM

	HCV	GAPDH
15: none	inactive	inactive
16: 1-CH_3	inactive	85.2
17: 2-CH_3	42.0	98.5
18: 3-CH_3	inactive	70.7
19: 4-CH_3	inactive	inactive
20: 7-CH_3	inactive	inactive
21: 8-CH_3	87.0	88.8
22: 9-CH_3	inactive	inactive
23: 10-CH_3	inactive	94.9

Figure 4. Anti-HCV activity of methyl-substituted regioisomers of *N*-butylphenanthridinone, **16–23**.

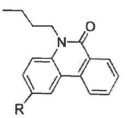

R	EC_{50} (μM)	CC_{50} (μM)
10: $(CF_3)_2(OH)C$-	3.7	12.5
15: H	>58.3	58.3
17: CH_3	35.8	38.4
24: F	>50	>50
25: OH	37.9	43.7
26: CF_3	>50	>50
27: CH_3CH_2	34.7	40.5
28: $(CH_3)_2CH$-	16.2	29.7
29: CH_2OH	21.5	>50
30: $CH_3CH(OH)$-	21.8	51.4
31: $(CH_3)_3CH$	10.6	24.9
32: CH_3CO-	18.7	27.3
33: $Ph(CH_2)_2$-	21.0	24.1

Figure 5. Anti-HCV activity of 2-substituted *N*-butylphenanthridinone, **15**, **17** and **24–33**.

Compounds **28–33** showed moderate anti-HCV activity (EC_{50}: 10.6–21.8 μM). Among the 2-alkylated derivatives, the activity decreased in the order of *t*-butyl (**31**) > *i*-propyl (**28**) > ethyl (**27**) > methyl (**17**), suggesting that the hydrophobicity of the 2-substituent contributes to the activity, at least in part. On the other hand, introduction of a hydroxyl group into the ethyl (**30**) or methyl (**29**) group of **27** and **17**, respectively, seemed to slightly enhance the activity, that is, **27** (EC_{50}: 34.7 μM) versus **30** (EC_{50}: 21.8 μM) and **17** (EC_{50}: 35.8 μM) versus **29** (EC_{50}: 21.5 μM). The 2-acetyl derivative **32** showed slightly more potent activity than **30**.

2.5. Tetrahydrotetramethylnaphthalene-related analogs and benzophenanthridinone analogs

Although the structure–activity relationships of 2-substituted *N*-butylphenanthridinone were clearly interpretable, hydrophobicity around the 2-position also seemed to contribute to the activity. This and the armchair structural development shown in Figure 1 prompted us to prepare compounds **34–38** (Fig. 6). We also prepared benzophenanthridinone derivatives **39–44** (Fig. 7). Among the tetrahydrotetramethylnaphthalene-related analogs **34–38**, only the *N*-butyl and *N*-benzyl derivatives (**35** and **36**, respectively) were moderately active, as shown in Figure 6. The regioisomer of **35**, that is, compound **38**, was inactive.

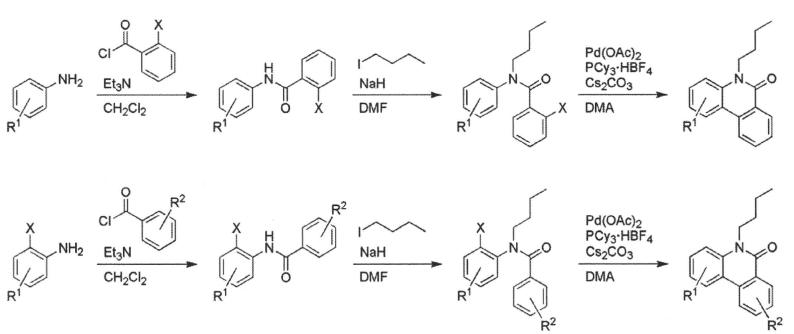

Scheme 3.

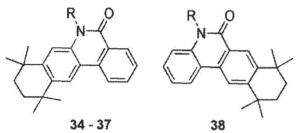

R	EC_{50} (μM)	CC_{50} (μM)
34: H	inactive	inactive
35: $CH_3(CH_2)_3$-	18.7	27.3
36: $PhCH_2$-	21.2	31.8
37: c-$C_6H_{11}CH_2$-	inactive	inactive
38: $CH_3(CH_2)_3$-	inactive	inactive

Figure 6. Anti-HCV activity of tetrahydrotetramethylnaphthalene-related analogs, **34–38**.

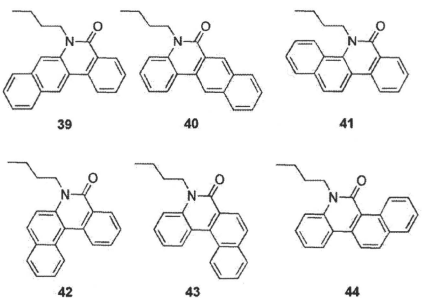

	EC_{50} (μM)	CC_{50} (μM)
35	18.7	27.3
39	3.2	6.3
40	11.0	>40
41	19.5	24.3
42	29.1	44.5
43	>31.4	31.4
44	29.9	>40

Figure 7. Anti-HCV activity of benzophenathridinone derivatives, **39–44**.

Benzophenanthridinone derivatives **39–44** were prepared as shown in Scheme 4. All the benzophenanthridinone derivatives, except **43**, showed potent or moderate anti-HCV activity. The activity decreased in the order of: benzo[*b*] (**39**) > benzo[*j*] (**40**) > benzo[*c*] (**41**) > benzo[*a*] (**42**) > benzo[*i*] (**44**) >> benzo[*k*] (**43**) as shown in Figures 7 and 8. Although compound **39** showed the most

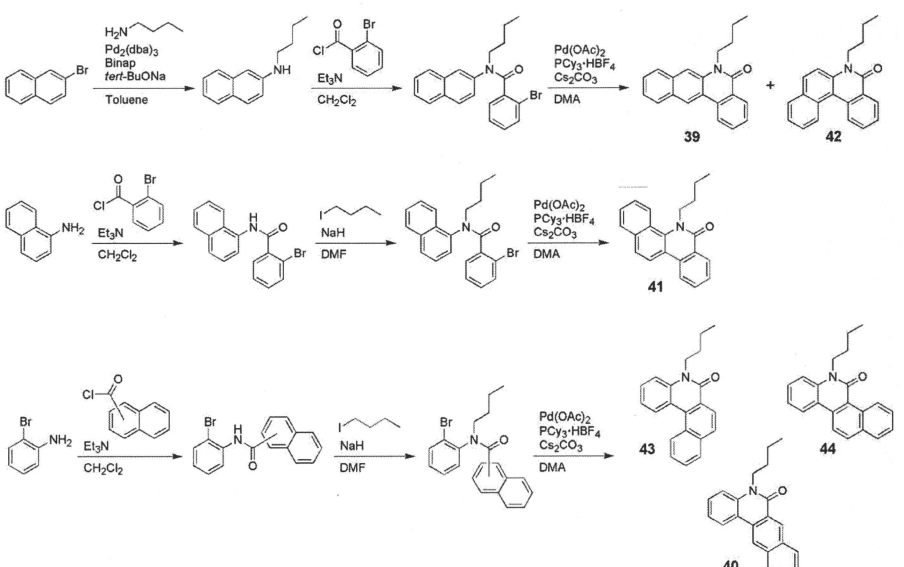

Scheme 4.

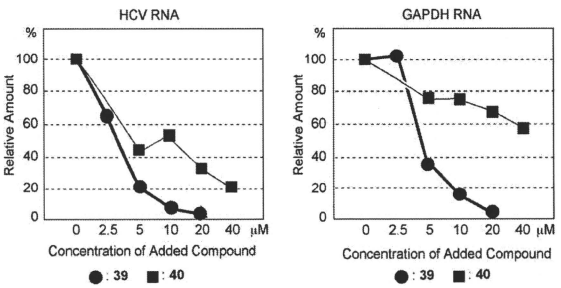

Figure 8. Dose-dependency curves of anti-HCV and cytotoxic activity elicited by compounds **39** and **40**.

potent anti-HCV activity (EC_{50}: 3.2 μM) among the compounds in this paper, its selectivity index (SI = CC_{50}/EC_{50}) was low (SI: 1.97). In terms of SI, compound **40** (EC_{50}: 11.0 μM) seems to be the best (SI: >3.64).

3. Conclusion

Based on a phenanthridinone skeleton derived by armchair structural development of thalidomide and retinoids, we developed candidate anti-HCV agents, **10** (EC_{50}: 3.7 μM,), **39** (EC_{50}: 3.2 μM,), and **40** (EC_{50}: 11 μM, CC_{50}: >40 μM). Further structural development may yield highly potent and selective drug candidates.

4. Experimental

4.1. General comments

Melting points were determined by using a Yanagimoto hot-stage melting point apparatus and are uncorrected. ^{1}H NMR spectra were recorded on a JEOL JNM-GX500 (500 MHz) spectrometer. Chemical shifts are expressed in δ (ppm) values with tetramethylsilane (TMS) as an internal reference. The following abbreviations are used: s = singlet, d = doublet, t = triplet, m = multiplet, dd = double doublet, dt = double triplet, br = broad. Mass spectra (MS) and high-resolution mass spectra (HRMS) were recorded on a JEOL JMS-DX303 spectrometer. Elemental analysis was performed with a Yanagimoto MT-6 elemental analyser.

4.2. 5-Ethyl-2-(1,1,1,3,3,3-hexafluoro-2-hydroxypropan-2-yl)-phenanthridin-6(5*H*)-one (8)

To a solution of 5 mmol of *N*-ethylaniline and 25 mL of toluene were added hexafluoroacetone trihydrate (1.2 equiv) and *p*-TsOH (0.1 equiv). The mixture was stirred for 22 h at 120 °C and the solvent was evaporated in vacuo. The residue was purified by silica gel column chromatography (eluent; *n*-hexane/ethyl acetate) to afford 2-(4-ethylaminophenyl)-1,1,1,3,3,3-hexafluoropropan-2-ol. The obtained compound was dissolved in dichloromethane (0.1 mmol/mL), and then triethylamine (1:40 v/v) and 2-iodobenzoyl chloride (1.2 equiv) were added. The mixture was stirred for 15 h at room temperature and the solvent was evaporated in vacuo. The residue was purified by silica gel column chromatography (eluent; *n*-hexane/ethyl acetate) to afford benzanilide derivatives. To a solution of the obtained benzanilide derivative, cesium carbonate (2 equiv) and *N,N*-dimethylacetamide were added palladium (II) acetate (10 mol %) and tricyclohexylphosphine tetrafluoroborate (0.15 equiv), and the mixture was heated to 130 °C. The catalyst was filtered off and washed several times with ethyl acetate. The combined organic layers were washed with water and brine successively, dried over anhydrous magnesium sulfate, and concentrated. The residue was purified by silica gel column chromatography (eluent; *n*-hexane/ethyl acetate) to afford 5-ethyl-2-(1,1,1,3,3,3-hexafluoro-2-hydroxypropan-2-yl)phenanthridin-6(5*H*)-one (**8**) as a white solid. Mp 208.0–209.0 °C. ^{1}H NMR (500 MHz, $CDCl_3$) δ 8.68 (d, J = 1.5 Hz, 1H), 8.56 (dd, J = 7.9, 1.5 Hz, 1H), 8.31 (d, J = 7.9 Hz, 1H), 7.85 (d, J = 9.4 Hz, 1H), 7.80 (td, J = 7.9, 1.3 Hz, 1H), 7.63 (t, J = 7.7 Hz, 1H), 7.50 (d, J = 9.0 Hz, 1H), 4.48 (q, J = 7.3 Hz, 2H), 3.71 (s, 1H), 1.44 (t, J = 7.3 Hz, 3H). HRMS (FAB) calcd for $C_{18}H_{14}F_6NO_2$ 390.0929; found: 390.0918 $(M+H)^+$.

4.3. 2-(1,1,1,3,3,3-Hexafluoro-2-hydroxypropan-2-yl)-5-(2,2,2-trifluoroethyl)phenanthridin-6(5*H*)-one (9)

The title compound was prepared by a method similar to that described for the synthesis of **8**, using aniline as a starting material, with slight modifications. 2-(4-Aminophenyl)-1,1,1,3,3,3-hexafluoropropan-2-ol (prepared from aniline and 1,1,1,3,3,3-hexafluoroacetone)[29] was coupled with 2-iodobenzoyl chloride, followed by protection of the hydroxyl group with 2-methoxylethoxymethyl chloride. It was then N-alkylated by the use of 2,2,2-trifluoroethyl triflate. The 2-methoxyethoxymethyl group of the obtained benzanilide derivative was removed by treatment with titanium tetrachloride, and the deprotected benzanilide derivative was cyclized by the method used for the synthesis of **8**. White solid. Mp 76.1–77.8 °C. ^{1}H NMR (500 MHz, $CDCl_3$) δ 8.70 (d, J = 1.1 Hz, 1H), 8.56 (dd, J = 8.1, 1.1 Hz, 1H), 8.33 (d, J = 8.1 Hz, 1H), 7.87 (dd, J = 7.7, 1.1 Hz, 1H), 7.85 (dd, J = 7.7, 1.1 Hz, 1H), 7.66 (td, J = 8.1 Hz, 1H), 7.51 (d, J = 9.0 Hz, 1H), 5.13 (s, 2H), 3.78 (s, 1H). HRMS (FAB) calcd for $C_{18}H_{10}F_9NO_2$ 444.0646; found: 444.0653 $(M+H)^+$.

4.4. 5-Butyl-2-(1,1,1,3,3,3-hexafluoro-2-hydroxypropan-2-yl)-phenanthridin-6(5*H*)-one (10)

The title compound was prepared by a method similar to that described for the synthesis of **9** using 1-iodobutane instead of 2,2,2-trifluoroethyl triflate. White solid. Mp 166.0–166.6 °C. ^{1}H NMR (500 MHz, $CDCl_3$) δ 8.67 (s, 1H), 8.55 (d, J = 7.9 Hz, 1H), 8.30 (d, J = 7.9 Hz, 1H), 7.84 (d, J = 7.9 Hz, 1H), 7.79 (dd, J = 7.9, 7.3 Hz, 1H), 7.62 (dd, J = 7.9, 7.3 Hz, 1H), 7.47 (d, J = 7.9 Hz, 1H), 4.39 (t, J = 7.9 Hz, 2H), 3.81 (s, 1H), 1.83–1.76 (m, 2H), 1.56–1.50 (m, 2H),

1.03 (t, J = 7.3 Hz, 3H). HRMS (FAB) calcd for $C_{20}H_{18}F_6NO_2$ 418.1242; found: 418.1262 $(M+H)^+$.

4.5. 2-(1,1,1,3,3,3-Hexafluoro-2-hydroxypropan-2-yl)-5-hexylphenanthridin-6(5*H*)-one (11)

The title compound was prepared by a method similar to that described for the synthesis of compound **9**, using 1-iodohexane instead of 2,2,2-trifluoroethyl triflate. White solid. Mp 132.0–132.2 °C. ^{1}H NMR (500 MHz, $CDCl_3$) δ 8.67 (d, J = 1.8 Hz, 1H), 8.54 (d, J = 7.9, 1.8 Hz, 1H), 8.29 (d, J = 7.9 Hz, 1H), 7.84 (d, J = 8.5 Hz, 1H), 7.78 (dd, J = 8.5, 7.3 Hz, 1H), 7.62 (dd, J = 8.5, 7.3 Hz, 1H), 7.46 (d, J = 8.5 Hz, 1H), 4.37 (t, J = 7.9 Hz, 2H), 3.91 (s, 1H), 1.84–1.76 (m, 2H), 1.53–1.47 (m, 2H), 1.42–1.32 (m, 4H), 0.91 (t, J = 7.3 Hz, 3H). HRMS (FAB) calcd for $C_{22}H_{22}F_6NO_2$ 446.1555; found: 446.1516 $(M+H)^+$.

4.6. 2-(1,1,1,3,3,3-Hexafluoro-2-hydroxypropan-2-yl)-5-nonylphenanthridin-6(5*H*)-one (12)

The title compound was prepared by a method similar to that described for the synthesis of compound **9**, using 1-bromononane instead of 2,2,2-trifluoroethyl triflate. White solid. Mp 98.1–99.0 °C. ^{1}H NMR (500 MHz, $CDCl_3$) δ 8.67 (d, J = 1.8 Hz, 1H), 8.54 (d, J = 7.9, 1.8 Hz, 1H), 8.29 (d, J = 7.9 Hz, 1H), 7.84 (d, J = 8.5 Hz, 1H), 7.79 (dd, J = 7.9, 7.3 Hz, 1H), 7.62 (dd, J = 7.9, 7.3 Hz, 1H), 7.46 (d, J = 8.5 Hz, 1H), 4.37 (t, J = 7.9 Hz, 2H), 3.87 (s, 1H), 1.84–1.76 (m, 2H), 1.53–1.46 (m, 2H), 1.43–1.36 (m, 2H), 1.33–1.24 (m, 8H), 0.88 (t, J = 7.3 Hz, 3H). HRMS (FAB) calcd for $C_{25}H_{28}F_6NO_2$ 488.2024; found: 488.1981 $(M+H)^+$.

4.7. 5-Benzyl-2-(1,1,1,3,3,3-hexafluoro-2-hydroxypropan-2-yl)-phenanthridin-6(5*H*)-one (13)

The title compound was prepared by a method similar to that described for the synthesis of compound **9**, using benzyl bromide instead of 2,2,2-trifluoroethyl triflate. White solid. Mp 80.0–80.9 °C. ^{1}H NMR (500 MHz, $CDCl_3$) δ 8.67 (d, J = 1.3 Hz, 1H), 8.63 (d, J = 8.1, 1.3 Hz, 1H), 8.34 (d, J = 8.1 Hz, 1H), 7.84 (td, J = 7.2, 1.3 Hz, 1H), 7.68 (q, J = 8.3 Hz, 2H), 7.38 (d, J = 9.4 Hz, 1H), 7.34–7.23 (m, 5H), 5.66 (s, 2H), 3.63 (s, 1H). HRMS (FAB) calcd for $C_{23}H_{15}F_6NO_2$ 452.1085; found: 452.1057 $(M+H)^+$. Anal. Calcd for $C_{23}H_{15}F_6NO_2 \cdot 1/3\ H_2O$: C, 60.40; H, 3.45; N, 3.06. Found: C, 60.46; H, 3.47; N, 3.08.

4.8. 5-(Cyclohexylmethyl)-2-(1,1,1,3,3,3-hexafluoro-2-hydroxypropan-2-yl)phenanthridin-6(5*H*)-one (14)

The title compound was prepared by a method similar to that described for the synthesis of compound **9**, using cyclohexylmethyl bromide instead of 2,2,2-trifluoroethyl triflate. White solid. Mp 200.9–201.7 °C. ^{1}H NMR (500 MHz, $CDCl_3$) δ 8.67 (d, J = 1.8 Hz, 1H), 8.55 (d, J = 8.5, 1.8 Hz, 1H), 8.30 (d, J = 8.5 Hz, 1H), 7.83 (d, J = 8.5 Hz, 1H), 7.79 (dd, J = 8.5, 7.3 Hz, 1H), 7.62 (dd, J = 8.5, 7.3 Hz, 1H), 7.46 (d, J = 8.5 Hz, 1H), 4.30 (br s, 2H), 3.75 (s, 1H), 1.98–1.88 (m, 1H), 1.76–1.64 (m, 5H), 1.24–1.17 (m, 5H). HRMS (FAB) calcd for $C_{23}H_{22}F_6NO_2$ 458.1555; found: 458.1569 $(M+H)^+$.

4.9. 5-Butylphenanthridin-6(5*H*)-one (15)

The title compound was prepared by a method similar to that described for the synthesis of **9**, using aniline as a starting material, with slight modifications, that is, 1-iodobutane was used in place of 2,2,2-trifluoroethyl triflate. Colorless oil. ^{1}H NMR (500 MHz, $CDCl_3$) δ 8.54 (dd, 1H, J = 7.9, 1.3 Hz), 8.29 (dd, 1H, J = 8.6, 1.3 Hz), 8.27 (d, 1H, J = 8.6 Hz), 7.74 (ddd, 1H, J = 8.0, 7.4, 1.2 Hz), 7.57 (t, 1H, J = 7.4, Hz), 7.53 (ddd, 1H, J = 8.5, 7.4, 1.2 Hz), 7.40 (d, 1H, J = 8.5 Hz), 7.30 (dd, 1H, J = 8.0, 7.4 Hz), 4.38 (t, 2H, J = 7.9, Hz), 1.78 (td, 2H, J = 7.9, 7.3 Hz), 1.52 (sextet, 2H, J = 7.3 Hz), 1.00 (t, 3H, J = 7.3, Hz). HRMS (FAB) calcd for $C_{17}H_{17}NO$ 252.1388; found: 252.1349 $(M+H)^+$.

4.10. 5-Butyl-1-methylphenanthridin-6(5*H*)-one (16)

The title compound was prepared by a method similar to that described for the synthesis of **15**, using 2-iodo-3-methylaniline as a starting material. Benzoyl chloride was used instead of 2-iodobenzoyl chloride. Pale brown oil. ^{1}H NMR (500 MHz, $CDCl_3$) δ 8.64 (d, 1H, J = 8.0 Hz), 8.44 (d, 1H, J = 8.0 Hz), 7.73 (t, 1H, J = 8.0 Hz), 7.59 (t, 1H, J = 8.0 Hz), 7.42 (t, 1H, J = 8.0 Hz), 7.33 (d, 1H, J = 8.0 Hz), 7.17 (d, 1H, J = 8.0 Hz), 4.40 (t, 2H, J = 7.6 Hz), 2.96 (s, 3H), 184–1.77 (m, 2H), 158–1.48 (m, 2H), 1.02 (t, 3H, J = 7.6 Hz). HRMS (FAB) calcd for $C_{18}H_{19}NO$ 266.1545; found: 266.1568 $(M+H)^+$.

4.11. 5-Butyl-2-methylphenanthridin-6(5*H*)-one (17)

The title compound was prepared by a method similar to that described for the synthesis of **15**, using 4-methylaniline as a starting material. 2-Bromobenzoyl chloride was used instead of 2-iodobenzoyl chloride. Colorless oil. ^{1}H NMR (500 MHz, $CDCl_3$) δ 8.55 (dd, 1H, J = 8.0, 1.2 Hz), 8.28 (d, 1H, J = 8.0 Hz), 8.10 (s, 1H), 7.74 (td, 1H, J = 8.0, 1.2 Hz), 7.57 (m, 1H), 7.37–7.30 (d, 1H, J = 7.6 Hz), 4.38 (t, 2H, J = 7.6 Hz), 2.49 (s, 3H), 1.82–1.75 (m, 3H), 1.56–1.48 (m, 2H), 1.01 (t, 3H, J = 7.3 Hz). HRMS (FAB) calcd for $C_{18}H_{19}NO$ 266.1545; found: 266.1584 $(M+H)^+$.

4.12. 5-Butyl-3-methylphenanthridin-6(5*H*)-one (18)

The title compound was prepared by a method similar to that described for the synthesis of **16**, using 2-bromo-5-methylaniline as a starting material. Pale brown oil. ^{1}H NMR (500 MHz, $CDCl_3$) δ 8.53 (d, 1H, J = 8.0 Hz), 8.24 (d, 1H, J = 8.0 Hz), 8.80 (d, 1H, J = 8.0 Hz), 7.73 (t, 1H, J = 8.0 Hz), 7.55 (t, 1H, J = 8.0 Hz), 7.20 (s, 1H), 7.13 (d, 1H, J = 8.0 Hz), 4.39 (t, 2H, J = 7.5 Hz), 2.52 (s, 3H), 1.83–1.76 (m, 2H), 1.57–1.49 (m, 2H), 1.03 (t, 3H, J = 7.5 Hz). HRMS (FAB) calcd for $C_{18}H_{19}NO$ 266.1545; found: 266.1512 $(M+H)^+$.

4.13. 5-Butyl-4-methylphenanthridin-6(5*H*)-one (19)

The title compound was prepared by a method similar to that described for the synthesis of **17**, using 2-methylaniline as a starting material. Colorless oil. ^{1}H NMR (500 MHz, $CDCl_3$) δ 8.50 (dd, 1H, J = 8.0, 1.2 Hz), 8.22 (d, 1H, J = 8.0 Hz), 8.13 (d, 1H, J = 8.0 Hz), 7.20 (td, 1H, J = 7.6, 1.4 Hz), 7.55 (t, 1H, J = 8.0 Hz), 7.30 (d, 1H, J = 7.6 Hz), 7.21 (t, 1H, J = 7.6 Hz), 4.49 (t, 2H, J = 7.6 Hz), 2.66 (s, 3H), 1.66–1.60 (m, 2H), 1.20–1.19 (m, 2H), 0.86 (t, 3H, J = 7.3 Hz). HRMS (FAB) calcd for $C_{18}H_{19}NO$ 266.1545; found: 266.1557 $(M+H)^+$.

4.14. 5-Butyl-7-methylphenanthridin-6(5*H*)-one (20)

The title compound was prepared by a method similar to that described for the synthesis of **16**, using 2-bromoaniline as a starting material. 2-Methylbenzoyl chloride was used instead of benzoyl chloride. White amorphous solid. ^{1}H NMR (500 MHz, $CDCl_3$) δ 8.27 (d, 1H, J = 7.5 Hz), 8.17 (d, 1H, J = 7.5 Hz), 7.58 (t, 1H, J = 7.5 Hz), 7.51 (t, 1H, J = 7.5 Hz), 7.35 (t, 1H, J = 7.5 Hz), 7.26 (t, 1H, J = 7.5 Hz), 4.31 (t, 2H, J = 8.0 Hz), 2.98 (s, 3H), 1.81–1.74 (m, 2H), 1.58–1.49 (m, 2H), 1.02 (t, 3H, J = 7.3 Hz). HRMS (FAB) calcd for $C_{18}H_{19}NO$ 266.1545; found: 266.1573 $(M+H)^+$.

4.15. 5-Butyl-8-methylphenanthridin-6(5*H*)-one (21)

The title compound was prepared by a method similar to that described for the synthesis of **20**. 3-Methylbenzoyl chloride was used instead of 2-methylbenzoyl chloride. White amorphous solid. ^{1}H NMR (500 MHz, $CDCl_3$) δ 8.36 (s, 1H), 8.28 (d, 1H, J = 8.0 Hz), 8.18 (d, 1H, J = 8.0 Hz), 7.58 (dd, 1H, J = 8.0, 1.8 Hz), 7.52 (t, 1H, J = 8.0 Hz), 7.41 (d, 1H, J = 8.0 Hz), 7.30 (t, 1H, J = 8.0 Hz), 4.40 (t, 2H, J = 8.0 Hz), 2.52 (s, 3H), 1.83–1.76 (m, 2H), 1.56–1.50 (m, 2H), 1.02 (t, 3H, J = 7.3 Hz). HRMS (FAB) calcd for $C_{18}H_{19}NO$ 266.1545; found: 266.1588 $(M+H)^+$.

4.16. 5-Butyl-9-methylphenanthridin-6(5*H*)-one (22)

The title compound was prepared by a method similar to that described for the synthesis of **20**. 4-Methylbenzoyl chloride was used instead of 2-methylbenzoyl chloride. White solid. Mp 70.0–73.0 °C. ^{1}H NMR (500 MHz, $CDCl_3$) δ 8.44 (d, 1H, J = 7.5 Hz), 8.30 (d, 1H, J = 7.5 Hz), 8.07 (s, 1H7.5), 7.53 (td, 1H, J = 7.5 Hz), 7.40 (d, 2H, J = 7.5 Hz), 7.30 (dd, 1H, J = 7.5 Hz), 4.39 (t, 2H, J = 8.0 Hz), 2.57 (s, 3H), 1.81.75 (m, 2H), 1.51.49 (m, 2H), 1.02 (t, 3H, J = 7.3 Hz). HRMS (FAB) calcd for $C_{18}H_{19}NO$ 266.1545; found: 266.1527 $(M+H)^+$.

4.17. 5-Butyl-10-methylphenanthridin-6(5*H*)-one (23)

The title compound was prepared by a method similar to that described for the synthesis of **20**. Colorless oil. ^{1}H NMR (500 MHz, $CDCl_3$) δ 8.53 (d, 1H, J = 8.0 Hz), 8.70 (dd, 1H, J = 8.0, 1.2 Hz), 7.61 (d, 1H, J = 8.0 Hz), 7.56–7.52 (m, 1H), 7.49 (d, 1H, J = 8.0 Hz), 7.46 (dd, 1H, J = 8.0, 1.2 Hz), 7.32–7.27 (m, 1H), 4.40 (t, 2H, J = 7.3 Hz), 2.97 (s, 3H), 1.85–1.78 (m, 2H), 1.50–1.50 (m, 2H), 1.02 (t, 3H, J = 7.3 Hz). HRMS (FAB) calcd for $C_{18}H_{19}NO$ 266.1545; found: 266.1553 $(M+H)^+$.

4.18. 5-Butyl-2-fluorophenanthridin-6(5*H*)-one (24)

The title compound was prepared by a method similar to that described for the synthesis of **17**, using 4-fluoroaniline as a starting material. White solid. FAB-MS m/z 270 $(M+H)^+$. Mp 114.0–117.5 °C. ^{1}H NMR (500 MHz, $CDCl_3$) δ 8.56 (dd, 1H, J = 8.0, 1.5 Hz), 8.17 (d, 1H, J = 8.0 Hz), 7.90 (dd, 1H, J = 9.7, 3.0 Hz), 7.77 (t, 1H, J = 8.0 Hz), 7.63 (t, 1H, J = 8.0 Hz), 7.37 (dd, 1H, J = 9.0, 4.5 Hz), 7.29–7.24 (m, 1H), 4.38 (t, 2H, J = 8.0 Hz), 1.82–1.75 (m, 2H), 1.57–1.48 (m, 2H), 1.02 (t, 3H, J = 7.3 Hz). Anal. Calcd for $C_{17}H_{16}NFO$: C, 75.82; H, 5.99; N, 5.20. Found: C, 76.22; H, 6.24; N, 5.24.

4.19. 5-Butyl-2-trifluoromethylphenanthridin-6(5*H*)-one (26)

The title compound was prepared by a method similar to that described for the synthesis of **17**, using 4-trifluoromethylaniline as a starting material. White solid. FAB-MS m/z 320 $(M+H)^+$. Mp 111.0–112.0 °C. ^{1}H NMR (500 MHz, $CDCl_3$) δ 8.56 (d, 1H, J = 8.0 Hz), 8.53 (s, 1H), 8.30 (d, 1H, J = 8.0 Hz), 7.82 (t, 1H, J = 8.0 Hz), 7.77 (dd, 1H, J = 8.0, 1.8 Hz), 7.65 (t, 1H, J = 8.0 Hz), 7.00 (d, 1H, J = 8.0 Hz), 4.41 (t, 2H, J = 7.9 Hz), 1.83–1.75 (m, 2H), 1.58–1.49 (m, 2H), 1.03 (t, 3H, J = 7.3 Hz). Anal. Calcd for $C_{18}H_{16}NF_3O$: C, 67.70; H, 5.05; N, 4.39. Found: C, 67.91; H, 5.33; N, 4.38.

4.20. 5-Butyl-2-ethylphenanthridin-6(5*H*)-one (27)

The title compound was prepared by a method similar to described that for the synthesis of **17**, using 4-ethylaniline as a starting material. Pale brown oil. ^{1}H NMR (500 MHz, $CDCl_3$) δ 8.55 (dd, 1H, J = 8.0, 1.5 Hz), 8.30 (d, 1H, J = 8.0 Hz), 8.12 (d, 1H, J = 1.5 Hz), 7.75 (td, 1H, J = 8.0, 1.5 Hz), 7.58 (t, 1H, J = 8.0 Hz), 7.39 (dd, 1H, J = 8.0, 1.5 Hz), 7.34 (d, 1H, J = 8.0 Hz), 4.39 (t, 2H, J = 8.0 Hz), 2.79 (q, 2H, J = 8.0 Hz), 1.83–1.76 (m, 2H), 1.57–1.49 (m, 2H), 1.34 (t, 3H, J = 7.6 Hz), 1.02 (t, 3H, J = 7.3 Hz). HRMS (FAB) calcd for $C_{19}H_{21}NO$ 280.1701; found: 280.1696 $(M+H)^+$.

4.21. 5-Butyl-2-isopropylphenanthridin-6(5*H*)-one (28)

The title compound was prepared by a method similar to that described for the synthesis of **15**, using 4-isopropylaniline as a starting material. Colorless oil. ^{1}H NMR (500 MHz, $CDCl_3$) δ 8.54 (dd, 1H, J = 8.0, 1.2 Hz), 8.30 (d, 1H, J = 8.0 Hz), 8.12 (d, 1H, J = 1.9 Hz), 7.74 (ddd, 1H, J = 7.9, 7.4, 1.2 Hz), 7.56 (dd, 1H, J = 8.0, 7.4 Hz), 7.41 (dd, 1H, J = 8.6, 1.9 Hz), 7.34 (d, 1H, J = 8.6 Hz), 4.37 (t, 2H, J = 8.0 Hz), 3.05 (septet, 1H, J = 7.4 Hz), 1.77 (quintet, 2H, J = 8.0 Hz), 1.51 (sextet, 2H, J = 7.4 Hz), 1.34 (d, 6H, J = 7.4 Hz), 1.00 (t, 3H, J = 7.4 Hz). HRMS (FAB) calcd for $C_{20}H_{23}NO$ 294.1858; found: 294.1851 $(M+H)^+$.

4.22. 5-Butyl-2-*tert*-butylphenanthridin-6(5*H*)-one (31)

The title compound was prepared by a method similar to that described for the synthesis of **17** using 4-*tert*-burylaniline as a starting material. Pale brown oil. ^{1}H NMR (500 MHz, $CDCl_3$) δ 8.56 (dd, 1H, J = 8.0, 1.5 Hz), 8.32 (d, 1H, J = 8.0 Hz), 8.31 (d, 1H, J = 1.5 Hz), 7.78–7.74 (m, 1H), 7.60 (dd, 1H, J = 8.0, 1.5 Hz), 7.57 (d, 1H, J = 8.0 Hz), 7.37 (d, 1H, J = 8.0 Hz), 4.39 (t, 2H, J = 7.6 Hz), 1.83–1.76 (m, 2H), 1.56–1.50 (m, 2H), 1.44 (s, 9H), 1.02 (t, 3H, J = 7.3 Hz). HRMS (FAB) calcd for $C_{21}H_{25}NO$ 308.2014; found: 308.2008 $(M+H)^+$.

4.23. 5-Butyl-2-hydroxyphenanthridin-6(5*H*)-one (25)

The title compound was prepared by a method similar to that described for the synthesis of **8**, using 4-*tert*-butyldimethylsilyloxyaniline (prepared from *p*-nitrophenol) as a starting material, with slight modifications. 4-*tert*-Butyldimethylsilyloxyaniline was acylated with butyryl chloride in the presence of triethylamine in dichloromethane, and then hydrogenated with lithium aluminum hydride in tetrahydrofuran. Obtained *N*-butylaniline was coupled with 2-iodobenzoyl chloride, and then cyclized in the presence of palladium (II) acetate, tricyclohexylphosphine tetrafluoroborate and potassium carbonate in *N*,*N*-dimethylacetamide. White solid. Mp 187.0–192.0 °C. ^{1}H NMR (500 MHz, $CDCl_3$) δ 8.55 (d, 1H, J = 7.9 Hz), 8.10 (d, 1H, J = 7.9 Hz), 7.78 (d, 1H, J = 2.4 Hz), 7.67 (t, 1H, J = 7.3 Hz), 7.55 (t, 1H, J = 7.3 Hz), 7.28 (d, 1H, J = 9.2 Hz), 7.14 (dd, 1H, J = 9.2, 2.4 Hz), 6.68 (br s, 1H), 4.37 (t, 2H, J = 7.3 Hz), 1.77 (quintet, 2H, J = 7.3 Hz), 1.49 (sextet, 2H, J = 7.3 Hz), 0.97 (t, 3H, J = 7.3 Hz). HRMS (FAB) calcd for $C_{17}H_{17}NO_2$ 268.1338; found: 268.1344 $(M+H)^+$.

4.24. 5-Butyl-2-hydroxymethylphenanthridin-6(5*H*)-one (29)

White solid. FAB-MS m/z 282 $(M+H)^+$. Mp 150.0–153.0 °C. ^{1}H NMR (500 MHz, $CDCl_3$) δ 18.54 (d, 1H, J = 8.0 Hz), 8.28–8.26 (m, 2H), 7.75 (t, 1H, J = 8.0 Hz), 7.59 (t, 1H, J = 8.0, 1.8 Hz), 7.52 (dd, 1H, J = 8.0, 1.8 Hz), 7.36 (d, 1H, J = 8.0 Hz), 4.83 (d, 2H, J = 6.0 Hz), 4.37 (t, 2H, J = 7.5 Hz), 1.99–1.94 (m, 1H), 1.81–1.74 (m, 2H), 1.55–1.48 (m, 2H), 1.01 (t, 3H, J = 7.5 Hz). Anal. Calcd for $C_{18}H_{19}NO_2$: C, 76.84; H, 6.81; N, 4.98. Found: C, 76.94; H, 6.71; N, 5.01.

4.25. 5-Butyl-2-(1′-hydroxyethyl)phenanthridin-6(5*H*)-one (30)

The title compound was prepared by a method similar to that described for the synthesis of **25**, using 1-(4-aminophenyl)ethanol as a starting material. Pale yellow solid. Mp 95.0–99.0 °C. ^{1}H NMR (500 MHz, $CDCl_3$) δ 8.51 (dd, 1H, J = 7.9, 1.2 Hz), 8.23 (d, 1H, J = 8.5 Hz), 8.22 (d, 1H, J = 1.8 Hz), 7.72 (td, 1H, J = 7.3, 1.2 Hz),

7.56 (dd, 1H, J = 7.9, 7.3 Hz), 7.49 (dd, 1H, J = 8.5, 1.8 Hz), 7.29 (d, 1H, J = 8.5 Hz), 5.03 (q, 1H, J = 6.7 Hz), 4.33 (t, 2H, J = 7.9 Hz), 1.74 (quintet, 2H, J = 7.9 Hz), 1.57 (d, 3H, J = 6.7 Hz), 1.49 (sextet, 2H, J = 7.3 Hz), 0.99 (t, 3H, J = 7.3 Hz). HRMS (FAB) calcd for $C_{19}H_{21}NO_2$ 296.1651; found: 296.1661 $(M+H)^+$.

4.26. 5-Butyl-2-acetylphenanthridin-6(5*H*)-one (32)

The title compound was prepared by the same method as described for the synthesis of **30**. The title compound was generated by partial oxidization of the alcoholic hydroxy group at the final cyclization step. White solid. Mp 114.0–118.0 °C. ^1H NMR (500 MHz, $CDCl_3$) δ 8.92 (d, 1H, J = 1.8 Hz), 8.53 (d, 1H, J = 7.3 Hz), 8.37 (d, 1H, J = 7.9 Hz), 8.10 (dd, 1H, J = 9.2, 1.8 Hz), 7.79 (t, 1H, J = 7.3 Hz), 7.61 (dd, 1H, J = 7.9, 7.3 Hz), 7.44 (d, 1H, J = 9.2 Hz), 4.39 (t, 2H, J = 7.9 Hz), 2.69 (s, 3H), 1.77 (quintet, 2H, J = 7.9 Hz), 1.52 (sextet, 2H, J = 7.3 Hz), 1.01 (t, 3H, J = 7.3 Hz). HRMS (FAB) calcd for $C_{19}H_{19}NO_2$ 294.1494; found: 294.1501 $(M+H)^+$.

4.27. 5-Butyl-2-phenethylphenanthridin-6(5*H*)-one (33)

Compound **29** was oxidized with manganese oxide in dichloromethane to give an aldehyde derivative, which was coupled by Wittig reaction to give a styryl derivative. This product was hydrogenated in the presence of palladium–carbon under a hydrogen atmosphere to give the title compound. Colorless oil. ^1H NMR (500 MHz, $CDCl_3$) δ 8.55 (dd, 1H, J = 8.0, 1.2 Hz), 8.22 (d, 1H, J = 8.0 Hz), 8.05 (s, 1H), 7.74 (ddd, 1H, J = 8.0, 6.5, 1.2 Hz), 7.58 (t, 1H, J = 8.0 Hz), 7.37–7.29 (m, 4H), 7.24–7.21 (m, 3H), 4.38 (t, 2H, J = 7.9 Hz), 3.09–2.99 (m, 4H), 1.82–1.76 (m, 2H), 1.55–1.49 (m, 2H), 1.02 (t, 3H, J = 7.3 Hz). HRMS (FAB) calcd for $C_{25}H_{26}NO$ 356.2014; found: 356.1995 $(M+H)^+$.

4.28. 6-Butyl-8,9,10,11-tetrahydro-8,8,11,11-tetramethylbenzo-[2,3-*b*]phenanthridin-5(6*H*)-one (35)

The title compound was prepared by a method similar to that described for the synthesis of **17**, using 2-amino-5,6,7,8-tetrahydro-5,5,8,8-tetramethylnaphthalene as a starting material. Colorless oil. ^1H NMR (500 MHz, $CDCl_3$) δ 8.52 (d, 1H, J = 8.0 Hz), 8.26 (d, 1H, J = 8.0 Hz), 8.21 (s, 1H), 7.73 (t, 1H, J = 8.0 Hz), 7.54 (t, 1H, J = 8.0 Hz), 7.31 (s, 1H), 4.39 (t, 2H, J = 7.3 Hz), 1.84–1.75 (m, 6H), 1.59–1.50 (m, 2H), 1.40 (s, 6H), 1.38 (s, 6H), 1.04 (t, 3H, J = 7.3 Hz). HRMS (FAB) calcd for $C_{25}H_{31}NO$ 362.2484; found: 362.2473 $(M+H)^+$.

4.29. 6-Benzyl-8,9,10,11-tetrahydro-8,8,11,11-tetramethylbenzo-[2,3-*b*]phenanthridin-5(6*H*)-one (36)

The title compound was prepared by a method similar to that described for the synthesis of **35**. N-Alkylation was performed by using benzyl bromide. White amorphous solid. ^1H NMR (500 MHz, $CDCl_3$) δ 8.60 (dd, 2H, J = 8.0, 1.5 Hz), 8.29 (d, 1H, J = 8.0 Hz), 8.18 (s, 1H), 7.79–7.75 (m, 1H), 7.58 (t, 1H, J = 8.0 Hz), 7.37–7.28 (m, 4H), 7.23 (s, 1H), 7.22 (t, 1H, J = 8.0 Hz), 5.65 (s, 2H), 1.69 (d, 4H, J = 1.2 Hz), 1.36 (s, 6H), 1.14 (s, 6H). HRMS (FAB) calcd for $C_{28}H_{29}NO$ 396.2327; found: 396.2296 $(M+H)^+$.

4.30. 6-Cyclohexylmethyl-8,9,10,11-tetrahydro-8,8,11,11-tetramethylbenzo[2,3-*b*]phenanthridin-5(6*H*)-one (37)

The title compound was prepared by a method similar to that described for the synthesis of **35**. N-Alkylation was performed by using cyclohexylmethyl bromide. White solid. Mp 148.0–153.0 °C. ^1H NMR (500 MHz, $CDCl_3$) δ 8.52 (dd, 2H, J = 8.0, 1.2 Hz), 8.27 (d, 1H, J = 8.0 Hz), 8.21 (s, 1H), 7.73 (td, 1H, J = 8.0, 1.2 Hz), 7.54 (td, 1H, J = 8.0, 1.2 Hz), 7.29 (s, 1H), 4.30 (br s, 2H), 1.94–1.89 (m, 1H), 1.78 (s, 4H), 1.76 (t, 4H, J = 13.00 Hz), 1.41 (s, 6H), 1.38 (s, 6H), 1.29–1.15 (m, 6H). HRMS (FAB) calcd for $C_{28}H_{35}NO$ 402.2797; found: 402.2791 $(M+H)^+$.

4.31. 5-Butyl-8,9,10,11-tetrahydro-8,8,11,11-tetramethylbenzo-[2,3-*j*]phenanthridin-6(5*H*)-one (38)

The title compound was prepared by a method similar to that described for the synthesis of **20**. 5,6,7,8-Tetrahydro-5,5,8,8-tetramethyl-2-naphthoyl chloride (prepared from 5,6,7,8-tetrahydro-5,5,8,8-tetramethylnaphthalene-2-carboxylic acid)[4] was used instead of 2-methylbenzoyl chloride. White solid. FAB-MS m/z 362 $(M+H)^+$. Mp 103.0–109.0 °C. ^1H NMR (500 MHz, $CDCl_3$) δ 8.51 (s, 1H), 8.29 (d, 1H, J = 7.9 Hz), 8.21 (s, 1H), 7.50 (t, 1H, J = 7.9 Hz), 7.38 (d, 1H, J = 7.9 Hz), 7.29 (t, 1H, J = 7.3 Hz), 4.38 (t, 2H, J = 7.6 Hz), 1.81–1.74 (m, 6H), 1.56–1.50 (m, 2H), 1.42 (s, 6H), 1.40 (s, 6H), 1.02 (t, 3H, J = 7.3 Hz). Anal. Calcd for $C_{25}H_{31}NO{\cdot}1/7\ H_2O$: C, 82.47; H, 8.66; N, 3.85. Found: C, 82.64; H, 8.76; N, 3.71.

4.32. 8,9,10,11-Tetrahydro-8,8,11,11-tetramethylbenzo[2,3-*b*]-phenanthridin-5(6*H*)-one (34)

The title compound was prepared by a method similar to that described for the synthesis of **35**, using 4-methoxybenzyl bromide instead of 1-iodobutane, followed by deprotection of the 4-methoxybenzyl group with trifluoroacetic acid. White solid. Mp 280 °C (decomp). ^1H NMR (500 MHz, $CDCl_3$) δ 9.27 (s, 1H), 8.51 (dd, 1H, J = 7.8, 1.3 Hz), 8.28 (t, 1H, J = 7.8 Hz), 8.14 (s, 1H), 7.78 (td, 1H, J = 7.8, 1.3 Hz), 7.57 (t, 1H, J = 7.8 Hz), 7.11 (s, 1H), 1.76 (s, 4H), 1.39 (s, 6H), 1.38 (s, 6H). HRMS (FAB) calcd for $C_{21}H_{23}NO$ 306.1858; found: 306.1817 $(M+H)^+$.

4.33. 6-Butylbenzo[*b*]phenanthridin-5(6*H*)-one (39)

The title compound was prepared by a method similar to that described for the synthesis of **8**, using 2-butylaminonaphthalene as a starting material. 2-Butylaminonaphthalene was prepared from 2-bromonaphthalene by coupling reaction with *n*-butylamine in the presence of tris(dibenzylidenacetone)dipalladium, sodium *tert*-butoxide and n-butylamine. 2-Bromobenzoyl chloride was used instead of 2-iodobenzoyl chloride. White solid. Mp 101.0–104.0 °C. ^1H NMR (500 MHz, $CDCl_3$) δ 8.90 (s, 1H), 8.57 (dd, 1H, J = 8.0, 1.8 Hz), 8.46 (d, 1H, J = 8.0 Hz), 7.98 (d, 1H, J = 8.0 Hz), 7.92 (d, 1H, J = 8.0 Hz), 7.82–7.78 (m, 1H), 7.73 (s, 1H), 7.62 (t, 1H, J = 7.3 Hz), 7.55 (t, 1H, J = 7.3 Hz), 7.48 (t, 1H, J = 7.3 Hz), 4.50 (t, 3H, J = 7.9 Hz), 1.92–1.85 (m, 2H), 1.63–1.52 (m, 2H), 1.06 (t, 3H, J = 7.3 Hz). HRMS (FAB) calcd for $C_{21}H_{19}NO$ 302.1545; found: 302.1555 $(M+H)^+$.

4.34. 5-Butylbenzo[*j*]phenanthridin-6(5*H*)-one (40)

The title compound was prepared by a method similar to that described for the synthesis of **20**. 2-Naphthoyl chloride was used instead of 2-methylbenzoyl chloride. White solid. Mp 111.0–115.0 °C. ^1H NMR (500 MHz, $CDCl_3$) δ 9.14 (s, 1H), 8.74 (s, 1H), 8.48 (dd, 1H, J = 8.0, 1.5 Hz), 8.09 (d, 1H, J = 8.0 Hz), 8.04 (d, 1H, J = 8.0 Hz), 7.63 (t, 1H, J = 8.0 Hz), 7.57 (d, 1H, J = 8.0 Hz), 7.54 (dd, 1H, J = 8.0, 1.5 Hz), 7.42 (d, 1H, J = 8.0 Hz), 7.35 (t, 1H, J = 8.0 Hz), 4.43 (t, 2H, J = 7.6 Hz), 1.87–1.80 (m, 2H), 1.58–1.52 (m, 2H). HRMS (FAB) calcd for $C_{21}H_{19}NO$ 302.1545; found: 302.1591 $(M+H)^+$.

4.35. 5-Butylbenzo[*c*]phenanthridin-6(5*H*)-one (41)

The title compound was prepared by a method similar to that described for the synthesis of **17**, using 1-aminonaphthlene as a